PHYSICAL REVIEW D **84,** 075014 (2011)

Collider signatures of the SO(5) × U(1) gauge-Higgs unification

Yutaka Hosotani, Minoru Tanaka, and Nobuhiro Uekusa
Department of Physics, Osaka University, Toyonaka, Osaka 560-0043, Japan
(Received 1 April 2011; published 17 October 2011)

Collider signatures of the $SO(5) \times U(1)$ gauge-Higgs unification model in the Randall-Sundrum warped space are explored. Gauge couplings of quarks and leptons receive small corrections from the fifth dimension whose effects are tested by the precision data. It is found that the forward-backward asymmetries in e^+e^- collisions on the Z pole are well explained in a wide range of the warp factor z_L, but the model is consistent with the branching fractions of Z decay only for large $z_L \gtrsim 10^{15}$. Kaluza-Klein (KK) spectra of gauge bosons, quarks, and leptons as well as gauge and Higgs couplings of low-lying KK excited states are determined. Right-handed quarks and leptons have larger couplings to the KK gauge bosons than left-handed ones. Production rates of Higgs bosons and KK states at the Tevatron, LHC, and International Linear Collider are evaluated. The first KK Z has a mass 1130 GeV with a width 422 GeV for $z_L = 10^{15}$. The current limit on the Z' production at the Tevatron and LHC indicates $z_L > 10^{15}$. A large effect of parity violation appears in the difference between the rapidity distributions of e^+ and e^- in the decay of the first KK Z. The first KK gauge bosons decay into light and heavy quarks evenly.

DOI: 10.1103/PhysRevD.84.075014 PACS numbers: 12.60.−i, 11.10.Kk, 11.15.−q, 14.80.Rt

I. INTRODUCTION

One of the biggest issues in current physics is to find the Higgs boson and pin down its properties. The mechanism of electroweak (EW) symmetry breaking is yet to be uncovered. It is not clear if the EW symmetry is spontaneously broken in a way described in the standard model (SM). The search for the Higgs boson is carried on at the Tevatron and LHC. The forthcoming result will tell us whether or not the SM scenario of the Higgs boson with a mass <200 GeV is correct.

Many alternative models have been proposed with new physics beyond the standard model. The most popular scenario in this category is supersymmetry hidden at the TeV scale. The Higgs boson is absent in the Higgsless model in which Kaluza-Klein (KK) modes of gauge bosons in the fifth dimension unitarize the theory [1,2], whereas the Higgs boson appears as a pseudo-Nambu-Goldstone boson in the little Higgs model [3–5]. In the gauge-Higgs unification scenario the Higgs boson is unified with 4D gauge fields, appearing as a part of the extra-dimensional component of gauge potentials.

In the present paper we focus on phenomenological implications and predictions of gauge-Higgs unification [6–12], particularly of the $SO(5) \times U(1)$ model in the Randall-Sundrum (RS) warped space [13–18]. The Higgs boson is nothing but a four-dimensional (4D) fluctuation mode of the Wilson line phase θ_H representing an Aharonov-Bohm phase in the fifth dimension. It has been shown in a class of the $SO(5) \times U(1)$ models that the energy density is minimized at $\theta_H = \pm\frac{1}{2}\pi$ [17] where the Higgs boson becomes absolutely stable. There emerges the H parity invariance. Among low energy particles only the Higgs boson is H parity odd, whereas all other SM particles are H parity even [19,20].

One immediate consequence is that Higgs bosons become the dark matter of the Universe. From the WMAP data the Higgs boson mass m_H is estimated around 70 GeV [19]. This value does not contradict with the LEP2 bound $m_H > 114$ GeV, as the ZZH coupling exactly vanishes. In collider experiments Higgs bosons can be produced in pairs. However, they appear as missing energies and momenta as they do not decay [21,22].

How can we test the model at colliders? We examine this question by analyzing the precision data of gauge couplings of quarks and leptons, Higgs pair production at LHC and the International Linear Collider (ILC), KK spectra of various fields, and production and decay of the first KK modes of gauge bosons at the Tevatron and LHC. The model has one free parameter, the warp factor z_L of the RS space. It will be found that the present data from colliders prefer large $z_L > 10^{15}$ whereas the Higgs mass ~70 GeV accounting for the dark matter is obtained with $z_L \sim 10^5$ in the current model. The production of the first KK mode of the Z boson with a mass around 1130 GeV and a width 422 GeV for $z_L = 10^{15}$ at LHC will be one of the robust signals of the model.

The $SO(5) \times U(1)$ gauge-Higgs unification model at $\theta_H = \pm\frac{1}{2}\pi$ has similarity to the Higgsless model in such processes as WW scattering at the tree level as the Higgs boson contribution is absent due to the vanishing WWH coupling [1]. It has been also discussed that the Higgs boson in the model has correspondence to the holographic pseudo-Goldstone boson [23,24], resembling the little Higgs model. The stable Higgs boson serving as dark matter has similarity to a second Higgs boson in the inert Higgs doublet model with new parity [25–28]. We would like to stress that the current model can make many definitive, quantitative predictions by starting from a concrete action, to be compared with other predictions [29–46].

The paper is organized as follows. The model is introduced in Sec. II, and KK expansions of various fields are summarized in Sec. III. In Sec. IV gauge couplings of quarks and leptons are determined, and are compared with the precision data for forward-backward asymmetries in e^+e^- annihilation on the Z resonance and partial decay widths of the Z boson. In Sec. V pair production of Higgs bosons at LHC and ILC is examined. The spectrum of KK towers of gauge bosons, quarks, and leptons is determined in Sec. VI. Couplings of quarks and leptons to KK gauge bosons are evaluated in Sec. VII. In Sec. VIII signals of the first KK Z boson at the Tevatron and LHC are discussed. Section IX is devoted to conclusions.

II. MODEL

The $SO(5)\times U(1)$ gauge-Higgs unification scenario was proposed by Agashe, Contino, and Pomarol [13]. We analyze phenomenological consequences of the model given in Refs. [18,20]. The model without leptons was introduced in Ref. [17]. It has been shown that the model has H parity invariance which leads to the stable Higgs boson [19,20].

The model is defined in the RS warped space with a metric

$$ds^2 = G_{MN}dx^M dx^N = e^{-2\sigma(y)}\eta_{\mu\nu}dx^\mu dx^\nu + dy^2, \quad (2.1)$$

where $\eta_{\mu\nu} = \mathrm{diag}(-1, 1, 1, 1)$, $\sigma(y)=\sigma(y+2L)=\sigma(-y)$, and $\sigma(y) = k|y|$ for $|y| \le L$. The Planck and TeV branes are located at $y = 0$ and $y = L$, respectively. The bulk region $0 < y < L$ is anti–de Sitter spacetime with a cosmological constant $\Lambda = -6k^2$. The warp factor $z_L \equiv e^{kL} \gg 1$ is a parameter to be specified. The KK mass scale is given by $m_{\mathrm{KK}} = \pi k/(z_L - 1) \sim \pi k z_L^{-1}$, which turns out 840–1470 GeV for $z_L = 10^5$–10^{15}.

The model consists of $SO(5)\times U(1)_X \times SU(3)_c$ gauge fields (A_M, B_M, G_M), bulk fermions Ψ_a, brane fermions $\hat{\chi}_{\alpha R}$, and brane scalar Φ. The bulk part of the action is given by

$$\begin{aligned} S_{\mathrm{bulk}} &= \int d^5x\sqrt{-G}\Big[-\mathrm{tr}\frac{1}{4}F^{(A)MN}F^{(A)}_{MN} - \frac{1}{4}F^{(B)MN}F^{(B)}_{MN} \\ &\quad - \mathrm{tr}\frac{1}{2}F^{(C)MN}F^{(C)}_{MN} + \sum_a i\bar{\Psi}_a\mathcal{D}(c_a)\Psi_a\Big], \\ \mathcal{D}(c_a) &= \Gamma^A e_A{}^M\Big(\partial_M + \frac{1}{8}\omega_{MBC}[\Gamma^B,\Gamma^C] - ig_A A_M \\ &\quad - ig_B Q_{Xa}B_M - ig_C Q^{\mathrm{color}}G_M\Big) - c_a\sigma'(y). \end{aligned} \quad (2.2)$$

The gauge fixing and ghost terms associated with the three gauge groups have been suppressed. $F^{(A)}_{MN} = \partial_M A_N - \partial_N A_M - ig_A[A_M, A_N]$, $F^{(B)}_{MN} = \partial_M B_N - \partial_N B_M$, and $F^{(C)}_{MN} = \partial_M G_N - \partial_N G_M - ig_C[G_M, G_N]$. $Q^{\mathrm{color}} = 1$ or 0 for quark or lepton multiplets, respectively. The $SO(5)$ gauge fields A_M are decomposed as $A_M = \sum_{a_L=1}^3 A_M^{a_L}T^{a_L} + \sum_{a_R=1}^3 A_M^{a_R}T^{a_R} + \sum_{\hat{a}=1}^4 A_M^{\hat{a}}T^{\hat{a}}$, where T^{a_L,a_R} (a_L, $a_R = 1, 2, 3$) and $T^{\hat{a}}$ ($\hat{a} = 1, 2, 3, 4$) are the generators of $SO(4) \simeq SU(2)_L \times SU(2)_R$ and $SO(5)/SO(4)$, respectively. In the fermion part $\bar{\Psi} = i\Psi^\dagger\Gamma^0$ and Dirac Γ^M matrices are given by

$$\begin{aligned} &\Gamma^\mu = \begin{pmatrix} & \sigma^\mu \\ \bar{\sigma}^\mu & \end{pmatrix}, \qquad \Gamma^5 = \begin{pmatrix} 1 & \\ & -1 \end{pmatrix}, \\ &\sigma^\mu = (1, \vec{\sigma}), \qquad \bar{\sigma}^\mu = (-1, \vec{\sigma}). \end{aligned} \quad (2.3)$$

All of the bulk fermions belong to the vector (**5**) representation of $SO(5)$. The c_a term in Eq. (2.2) gives a bulk kink mass, where $\sigma'(y) = k\epsilon(y)$ is a periodic step function with a magnitude k. The dimensionless parameter c_a plays an important role in controlling profiles of fermion wave functions.

The orbifold boundary conditions at $y_0 = 0$ and $y_1 = L$ are given by

$$\begin{aligned} \begin{pmatrix} A_\mu \\ A_y \end{pmatrix}(x, y_j - y) &= P_j\begin{pmatrix} A_\mu \\ -A_y \end{pmatrix}(x, y_j + y)P_j^{-1}, \\ \begin{pmatrix} B_\mu \\ B_y \end{pmatrix}(x, y_j - y) &= \begin{pmatrix} B_\mu \\ -B_y \end{pmatrix}(x, y_j + y), \\ \Psi_a(x, y_j - y) &= P_j\Gamma^5\Psi_a(x, y_j + y), \\ P_j &= \mathrm{diag}(-1, -1, -1, -1, +1). \end{aligned} \quad (2.4)$$

The $SO(5)\times U(1)_X$ symmetry is reduced to $SO(4)\times U(1)_X \simeq SU(2)_L \times SU(2)_R \times U(1)_X$ by the orbifold boundary conditions. It is known that various orbifold boundary conditions fall into a finite number of equivalence classes of boundary conditions [8,47,48]. The physical symmetry of the true vacuum in each equivalence class of boundary conditions is dynamically determined at the quantum level.

The 4D Higgs field, which is a doublet both in $SU(2)_L$ and in $SU(2)_R$, appears as a zero mode in the $SO(5)/SO(4)$ part of the fifth-dimensional component of the vector potential $A_y^{\hat{a}}(x, y)$. Without loss of generality one assumes $\langle A_y^{\hat{a}}\rangle \propto \delta^{a4}$ when the EW symmetry is spontaneously broken. The zero modes of $A_y^{\hat{a}}$ ($a = 1, 2, 3$) are absorbed by W and Z bosons. The Wilson line phase θ_H is given by

$$\exp\Big\{\frac{i}{2}\theta_H \cdot 2\sqrt{2}T^{\hat{4}}\Big\} = \exp\Big\{ig_A\int_0^L dy\langle A_y\rangle\Big\}. \quad (2.5)$$

The 4D neutral Higgs field $H(x)$ appears as [39]

$$\begin{aligned} A_y^{\hat{4}}(x, y) &= \{\theta_H f_H + H(x)\}u_H(y) + \cdots, \\ f_H &= \frac{2}{g_A}\sqrt{\frac{k}{z_L^2 - 1}} = \frac{2}{g_w}\sqrt{\frac{k}{L(z_L^2 - 1)}}. \end{aligned} \quad (2.6)$$

Here the wave function of the 4D Higgs boson is given by $u_H(y) = [2k/(z_L^2 - 1)]^{1/2}e^{2ky}$ for $0 \le y \le L$

and $u_H(-y) = u_H(y) = u_H(y + 2L)$. $g_w = g_A/\sqrt{L}$ is the dimensionless 4D $SU(2)_L$ coupling.

For each generation two vector multiplets Ψ_1 and Ψ_2 for quarks and two vector multiplets Ψ_3 and Ψ_4 for leptons are introduced. Each vector multiplet, Ψ, is decomposed into one $(\frac{1}{2}, \frac{1}{2})$, $\check{\Psi}$, and one (0, 0) of $SU(2)_L \times SU(2)_R$. We denote Ψ_a's, for the third generation, as

$$\begin{aligned}
&\Psi_1 = (\check{\Psi}_1, t')_{2/3}, \quad \check{\Psi}_1 = \begin{pmatrix} T & t \\ B & b \end{pmatrix} \equiv (Q_1, q), \\
&\Psi_2 = (\check{\Psi}_2, b')_{-1/3}, \quad \check{\Psi}_2 = \begin{pmatrix} U & X \\ D & Y \end{pmatrix} \equiv (Q_2, Q_3), \\
&\Psi_3 = (\check{\Psi}_3, \tau')_{-1}, \quad \check{\Psi}_3 = \begin{pmatrix} \nu_\tau & L_{1X} \\ \tau & L_{1Y} \end{pmatrix} \equiv (\ell, L_1), \\
&\Psi_4 = (\check{\Psi}_4, \nu'_\tau)_0, \quad \check{\Psi}_4 = \begin{pmatrix} L_{2X} & L_{3X} \\ L_{2Y} & L_{3Y} \end{pmatrix} \equiv (L_2, L_3).
\end{aligned} \tag{2.7}$$

Subscripts 2/3, etc., represent $U(1)_X$ charges, Q_X, of Ψ_a's. q, Q_j, ℓ, and L_j are $SU(2)_L$ doublets. The electromagnetic charge $Q_{\rm EM}$ is given by

$$Q_{\rm EM} = T^{3_L} + T^{3_R} + Q_X. \tag{2.8}$$

Each Ψ_a has its bulk mass parameter c_a. Consistent results are obtained by taking $c_1 = c_2 \equiv c_q$ and $c_3 = c_4 \equiv c_\ell$ for each generation.

The additional brane fields are introduced on the Planck brane at $y = 0$. The brane scalar field Φ belongs to $(0, \frac{1}{2})$ of $SU(2)_L \times SU(2)_R$ with $Q_X = -\frac{1}{2}$, whereas the right-handed brane fermions $\hat{\chi}^q_{\alpha R}$ and $\hat{\chi}^\ell_{\alpha R}$ belong to $(\frac{1}{2}, 0)$. The brane fermions are

$$\begin{aligned}
&\hat{\chi}^q_{1R} = \begin{pmatrix} \hat{T}_R \\ \hat{B}_R \end{pmatrix}_{7/6}, \qquad \hat{\chi}^q_{2R} = \begin{pmatrix} \hat{U}_R \\ \hat{D}_R \end{pmatrix}_{1/6}, \\
&\hat{\chi}^q_{3R} = \begin{pmatrix} \hat{X}_R \\ \hat{Y}_R \end{pmatrix}_{-5/6}, \qquad \hat{\chi}^\ell_{1R} = \begin{pmatrix} \hat{L}_{1XR} \\ \hat{L}_{1YR} \end{pmatrix}_{-3/2}, \\
&\hat{\chi}^\ell_{2R} = \begin{pmatrix} \hat{L}_{2XR} \\ \hat{L}_{2YR} \end{pmatrix}_{1/2}, \qquad \hat{\chi}^\ell_{3R} = \begin{pmatrix} \hat{L}_{3XR} \\ \hat{L}_{3YR} \end{pmatrix}_{-1/2}.
\end{aligned} \tag{2.9}$$

Subscripts 7/6, etc., represent Q_X charges of $\hat{\chi}_R$'s. The brane part of the action is given by

$$\begin{aligned}
S_{\rm brane} = \int d^5x\sqrt{-G}\delta(y)\Big\{&-(D_\mu\Phi)^\dagger D^\mu\Phi - \lambda_\Phi(\Phi^\dagger\Phi - w^2)^2 + \sum_{\alpha=1}^{3}(\hat{\chi}^{q\dagger}_{\alpha R} i\bar{\sigma}^\mu D_\mu \hat{\chi}^q_{\alpha R} + \hat{\chi}^{\ell\dagger}_{\alpha R} i\bar{\sigma}^\mu D_\mu \hat{\chi}^\ell_{\alpha R}) \\
&- i[\kappa^q_1 \hat{\chi}^{q\dagger}_{1R}\check{\Psi}_{1L}\tilde{\Phi} + \tilde{\kappa}^q \hat{\chi}^{q\dagger}_{2R}\check{\Psi}_{1L}\Phi + \kappa^q_2 \hat{\chi}^{q\dagger}_{2R}\check{\Psi}_{2L}\tilde{\Phi} + \kappa^q_3 \hat{\chi}^{q\dagger}_{3R}\check{\Psi}_{2L}\Phi - ({\rm H.c.})] \\
&- i[\tilde{\kappa}^\ell \hat{\chi}^{\ell\dagger}_{3R}\check{\Psi}_{3L}\tilde{\Phi} + \kappa^\ell_1 \hat{\chi}^{\ell\dagger}_{1R}\check{\Psi}_{3L}\Phi + \kappa^\ell_2 \hat{\chi}^{\ell\dagger}_{2R}\check{\Psi}_{4L}\tilde{\Phi} + \kappa^\ell_3 \hat{\chi}^{\ell\dagger}_{3R}\check{\Psi}_{4L}\Phi - ({\rm H.c.})]\Big\}, \\
D_\mu\Phi = \Big(\partial_\mu - ig_A &\sum_{a_R=1}^{3} A^{a_R}_\mu T^{a_R} + i\frac{1}{2}g_B B_\mu\Big)\Phi, \qquad \tilde{\Phi} = i\sigma_2\Phi^*, \\
D_\mu\hat{\chi} = \Big(\partial_\mu - ig_A &\sum_{a_L=1}^{3} A^{a_L}_\mu T^{a_L} - iQ_X g_B B_\mu - ig_C Q^{\rm color} G_\mu\Big)\hat{\chi}.
\end{aligned} \tag{2.10}$$

The action $S_{\rm brane}$ is manifestly invariant under $SU(2)_L \times SU(2)_R \times U(1)_X$. The Yukawa couplings above exhaust all possible ones preserving the symmetry.

The nonvanishing vacuum expectation value $\langle\Phi^t\rangle = (0, w)$ has two important consequences. It is assumed only that $w \gg m_{\rm KK}$. First the $SU(2)_R \times U(1)_X$ symmetry is spontaneously broken down to $U(1)_Y$ and the zero modes of four-dimensional gauge fields of $SU(2)_R \times U(1)_X$ become massive except for the $U(1)_Y$ part. They acquire masses of $O(m_{\rm KK})$ as a result of the effective change of boundary conditions for low-lying modes in the Kaluza-Klein towers. Second the nonvanishing vacuum expectation value w induces mass couplings between brane fermions and bulk fermions:

$$\begin{aligned}
S^{\rm mass}_{\rm brane} = \int d^5x\sqrt{-G}\delta(y)\Big\{&-\sum_{\alpha=1}^{3} i\mu^q_\alpha(\hat{\chi}^{q\dagger}_{\alpha R}Q_{\alpha L} - Q^\dagger_{\alpha L}\hat{\chi}^q_{\alpha R}) - i\tilde{\mu}^q(\hat{\chi}^{q\dagger}_{2R}q_L - q^\dagger_L\hat{\chi}^q_{2R}) \\
&- \sum_{\alpha=1}^{3} i\mu^\ell_\alpha(\hat{\chi}^{\ell\dagger}_{\alpha R}L_{\alpha L} - L^\dagger_{\alpha L}\hat{\chi}^\ell_{\alpha R}) - i\tilde{\mu}^\ell(\hat{\chi}^{\ell\dagger}_{3R}\ell_L - \ell^\dagger_L\hat{\chi}^\ell_{3R})\Big\}, \\
\frac{\mu^q_\alpha}{\kappa^q_\alpha} = \frac{\tilde{\mu}^q}{\tilde{\kappa}^q} = \frac{\mu^\ell_\alpha}{\kappa^\ell_\alpha} = \frac{\tilde{\mu}^\ell}{\tilde{\kappa}^\ell} &= w.
\end{aligned} \tag{2.11}$$

Assuming that all $\mu^2 \gg m_{\rm KK}$, all of the exotic zero modes of the bulk fermions acquire large masses of $O(m_{\rm KK})$. It has been shown that all of the 4D anomalies associated with $SU(2)_L \times SU(2)_R \times U(1)_X$ gauge symmetry are canceled [18]. The $SU(2)_L \times U(1)_Y$ is further broken down to $U(1)_{\rm EM}$ by the Hosotani mechanism. The spectrum of the resultant light particles is the same as in the standard model. The generation mixing can be explained by considering matrix couplings of κ_j and $\tilde{\kappa}$, particularly of κ_2^q, $\tilde{\kappa}^q$, κ_3^l, $\tilde{\kappa}^l$.

The parameters of the model relevant for low energy physics are k, $z_L = e^{kL}$, g_A, g_B, the bulk mass parameters (c_q, c_ℓ), and the brane mass ratios $(\tilde{\mu}^q/\mu_2^q, \tilde{\mu}^\ell/\mu_3^\ell)$. All other parameters are irrelevant at low energies, provided that w, μ^2's are much larger than $m_{\rm KK}$. The value of θ_H is determined dynamically to be $\pm\frac{1}{2}\pi$ where the EW symmetry is spontaneously broken [20]. Three of the four parameters k, $z_L = e^{kL}$, g_A, g_B are determined from the Z boson mass m_Z, the weak gauge coupling g_w, and the Weinberg angle $\sin^2\theta_W$. The one parameter, say, z_L remains free.

When the generation mixing is turned off in the fermion sector, the bulk mass c_q and the ratio $\tilde{\mu}^q/\mu_2^q$ in each generation are determined from the two quark masses, and c_ℓ and $\tilde{\mu}^\ell/\mu_3^\ell$ from the two lepton masses. As $m_{\nu_e} \ll m_e$, all of the results discussed below do not depend on the unknown value of m_{ν_e} very much. The generation mixing can be incorporated by considering 3-by-3 matrices for the brane couplings κ's, or equivalently for the brane masses μ's.

Once the value of z_L is specified, all the relevant parameters of the model are determined. The spectra of particles and their KK towers, their wave functions in the fifth dimension, and all interaction couplings can be predicted. The mass of the 4D Higgs boson, m_H, is determined from the effective potential $V_{\rm eff}(\theta_H)$. It was found that m_H is about 70–135 GeV for $z_L = 10^5 \sim 10^{15}$ [20]. Conversely the remaining one parameter z_L is fixed, once the Higgs boson mass m_H is given.

As typical reference values we take the warp factors $z_L = 10^5$, 10^{10}, 10^{15}. The values in Table I are taken as input parameters. The masses of quarks and charged leptons except for the t quark are quoted from Ref. [49]. The masses of Z boson and t quark are the central values in the Particle Data Group review [50]. The couplings α and α_s are also quoted from Ref. [50]. In the present analysis, the neutrino masses have negligible effects.

The parameter $\sin^2\theta_W$ is determined from the χ^2 fit of forward-backward asymmetries in e^+e^- annihilation and branching ratios in the Z decay as explained below. We find the best fit with $\sin^2\theta_W = 0.2284, 0.2303, 0.2309$ for $z_L = 10^5$, 10^{10}, 10^{15}, respectively. Since complete one-loop analysis is not available in the gauge-Higgs unification scenario at the moment, there remains ambiguity in the value of $\sin^2\theta_W$.

TABLE I. Input parameters for the masses and couplings of the model. The masses are in units of GeV. All masses except for m_t are at the m_Z scale.

m_Z	91.1876
m_u	1.27×10^{-3}
m_c	0.619
m_t	171.17
m_d	2.90×10^{-3}
m_s	0.055
m_b	2.89
$\alpha_s(m_Z)$	0.1176
m_{ν_e}	1×10^{-12}
m_{ν_μ}	9×10^{-12}
m_{ν_τ}	5.0309×10^{-11}
m_e	$0.486\,570\,161 \times 10^{-3}$
m_μ	$102.718\,135\,9 \times 10^{-3}$
m_τ	1.74624

III. KALUZA-KLEIN EXPANSION

With the orbifold boundary condition (2.4) the effective potential $V_{\rm eff}(\theta_H)$ is minimized at $\theta_H = \frac{1}{2}\pi$. To develop perturbation theory around $\theta_H = \frac{1}{2}\pi$, it is most convenient to move to the twisted gauge $\tilde{A}_M = \Omega A_M \Omega^{-1} + (i/g_A)\Omega\partial_M\Omega^{-1}$ in which $\langle\tilde{A}_y\rangle = 0$, or $\tilde{\theta}_H = 0$. We choose Ω preserving the boundary condition at the TeV brane:

$$\Omega(y) = \exp\left\{\frac{i\pi g_A f_H}{2}\int_y^L dy' u_H(y')\cdot T^{\hat{4}}\right\}. \tag{3.1}$$

In the twisted gauge the orbifold boundary condition $\{P_0, P_1\}$ is changed to $\{\tilde{P}_0, \tilde{P}_1\}$ where

$$\begin{aligned}\tilde{P}_0 &= \Omega(-y)P_0\Omega(y)^{-1} = \mathrm{diag}(-1,-1,-1,+1,-1) \neq P_0,\\ \tilde{P}_1 &= \Omega(L-y)P_1\Omega(L+y)^{-1}\\ &= \mathrm{diag}(-1,-1,-1,-1,+1) = P_1.\end{aligned} \tag{3.2}$$

The two sets $\{P_0, P_1\}$ and $\{\tilde{P}_0, \tilde{P}_1\}$ are in the same equivalence class of boundary conditions [8,47,48,51]. Although the boundary conditions are different, physics remains the same as a result of dynamics of the Wilson line phase. Note that $\Omega(L) = 1$, but

$$\Omega(0) = \begin{pmatrix} 1 & & & & \\ & 1 & & & \\ & & 1 & & \\ & & & 0 & 1 \\ & & & -1 & 0 \end{pmatrix} \tag{3.3}$$

so that the brane interactions take more complicated form than in the original gauge.

In the previous paper it was shown that the model has H parity (P_H) invariance, and H parity is assigned to all

4D fields [20]. P_H interchanges $SU(2)_L$ and $SU(2)_R$ and flips the sign of $T^{\hat{4}}$ in the bulk. P_H transformation is generated by $T^\alpha \to \Omega_H T^\alpha \Omega_H^{-1}$ where $\Omega_H = \mathrm{diag}(1, 1, 1, -1, 1)$ in the twisted gauge. The P_H symmetry is similar to the P_{LR} symmetry discussed by Agashe, Contino, Da Rold, and Pomarol [32], which protects the T parameter and $Zb\bar{b}$ coupling from radiative corrections. The neutral Higgs boson is the lightest particle of odd P_H so that it becomes stable.

In the twisted gauge the four-dimensional components of gauge fields are expanded as

$$\begin{aligned}
\tilde{A}_\mu(x,z) &= \hat{W}_\mu + \hat{W}_\mu^\dagger + \hat{Z}_\mu + \hat{A}_\mu^\gamma + \hat{W}'_\mu + \hat{W}'^\dagger_\mu + \hat{Z}'_\mu + \hat{A}_\mu^{\hat{4}},\\
\hat{W}_\mu &= \sum_n W_\mu^{(n)}\{h^L_{W^{(n)}} T^{-_L} + h^R_{W^{(n)}} T^{-_R} + h^\wedge_{W^{(n)}} T^{\hat{-}}\},\\
\hat{Z}_\mu &= \sum_n Z_\mu^{(n)}\{h^L_{Z^{(n)}} T^{3_L} + h^R_{Z^{(n)}} T^{3_R} + h^\wedge_{Z^{(n)}} T^{\hat{3}}\},\\
\hat{A}^\gamma_\mu &= \sum_n A_\mu^{\gamma(n)}\{h^L_{\gamma^{(n)}} T^{3_L} + h^R_{\gamma^{(n)}} T^{3_R}\},\\
\hat{W}'_\mu &= \sum_n W_\mu^{\prime(n)}\{h^L_{W'^{(n)}} T^{-_L} + h^R_{W'^{(n)}} T^{-_R}\},\\
\hat{Z}'_\mu &= \sum_n Z_\mu^{\prime(n)}\{h^L_{Z'^{(n)}} T^{3_L} + h^R_{Z'^{(n)}} T^{3_R}\},\\
\hat{A}^{\hat{4}}_\mu &= \sum_n A_\mu^{\hat{4}(n)} h_{A^{(n)}} T^{\hat{4}},\\
\tilde{B}_\mu(x,z) &= \sum_n Z_\mu^{(n)} h^B_{Z^{(n)}} + \sum_n A_\mu^{\gamma(n)} h^B_{\gamma^{(n)}}.
\end{aligned} \tag{3.4}$$

Here $T^\pm = (T^1 \pm iT^2)/\sqrt{2}$. The W and Z bosons and the photon γ correspond to $W_\mu^{(0)}$, $Z_\mu^{(0)}$, and $A_\mu^{\gamma(0)}$, respectively. Unless confusion arises, we will omit the superscript (0) for representing the lowest mode. The mixing angle between $SO(5)$ and $U(1)_X$ is related to the Weinberg angle by $\sin^2\theta_W \equiv s_\phi^2/(1+s_\phi^2)$ where $s_\phi = g_B/\sqrt{g_A^2 + g_B^2}$. All mode functions $h(z)$ are tabulated in the Appendix. They are expressed in terms of Bessel functions

$$\begin{aligned}
C(z;\lambda) &= \frac{\pi}{2}\lambda z z_L F_{1,0}(\lambda z, \lambda z_L),\\
C'(z;\lambda) &= \frac{\pi}{2}\lambda^2 z z_L F_{0,0}(\lambda z, \lambda z_L),\\
S(z;\lambda) &= -\frac{\pi}{2}\lambda z F_{1,1}(\lambda z, \lambda z_L),\\
S'(z;\lambda) &= -\frac{\pi}{2}\lambda^2 z F_{0,1}(\lambda z, \lambda z_L),\\
F_{\alpha,\beta}(u,v) &= J_\alpha(u) Y_\beta(v) - Y_\alpha(u) J_\beta(v).
\end{aligned} \tag{3.5}$$

For the photon ($\lambda_0 = 0$), $h^L_{\gamma^{(0)}} = h^R_{\gamma^{(0)}}$ is constant.

The mass spectrum $m_n = k\lambda_n$ of each KK tower is determined by the corresponding eigenvalue equations:

$$\begin{aligned}
&W_\mu^{(n)}\text{: } 2S(1;\lambda_n)C'(1;\lambda_n) + \lambda_n = 0,\\
&Z_\mu^{(n)}\text{: } 2S(1;\lambda_n)C'(1;\lambda_n) + \lambda_n(1+s_\phi^2) = 0,\\
&W_\mu^{\prime(n)}, Z_\mu^{\prime(n)}\text{: } C(1;\lambda_n) = 0, \qquad A_\mu^{\gamma(n)}\text{: } C'(1;\lambda_n) = 0,\\
&A_\mu^{\hat{4}(n)}\text{: } S(1;\lambda_n) = 0.
\end{aligned} \tag{3.6}$$

The Weinberg angle θ_W is determined by global fit of various quantities. In the present paper $\sin^2\theta_W$ is determined from the χ^2 fit of forward-backward asymmetries in e^+e^- annihilation and Z boson decay. With m_Z and z_L as an input, the anti–de Sitter curvature k and the W boson mass at the tree level, m_W^{tree}, are determined.

Similarly the fifth-dimensional components A_z and B_z are expanded as

$$\begin{aligned}
\tilde{A}_z(x,z) &= \sum_{a=1}^{3}\sum_{n=1}^{\infty} S^{a(n)} h_S^{LR}(\lambda_n)\frac{T^{a_L} + T^{a_R}}{\sqrt{2}} + \sum_{n=0}^{\infty} H^{(n)} h_H^\wedge(\lambda_n) T^{\hat{4}}\\
&\quad + \sum_{a=1}^{3}\sum_{n=1}^{\infty} D_-^{a(n)} h_D^{LR}(\lambda_n)\frac{T^{a_L} - T^{a_R}}{\sqrt{2}}\\
&\quad + \sum_{a=1}^{3}\sum_{n=1}^{\infty} \hat{D}^{a(n)} h_D^\wedge(\lambda_n) T^{\hat{a}},\\
\tilde{B}_z(x,z) &= \sum_{n=1}^{\infty} B^{(n)} h_B(\lambda_n).
\end{aligned} \tag{3.7}$$

$H(x) = H^{(0)}(x)$ is the 4D neutral Higgs boson. The mass spectrum of each KK tower is given by

$$\begin{aligned}
&S^{a(n)}, B^{(n)}\text{: } C'(1;\lambda_n) = 0, \qquad D_-^{a(n)}\text{: } C(1;\lambda_n) = 0,\\
&\hat{D}^{a(n)}\text{: } S'(1;\lambda_n) = 0, \qquad H^{(n)}\text{: } S(1;\lambda_n) = 0.
\end{aligned} \tag{3.8}$$

For the bulk fields H parity is assigned from the behavior under the transformation $\{T^{a_L}, T^{a_R}, T^{\hat{a}}, T^{\hat{4}}\} \to \{T^{a_R}, T^{a_L}, T^{\hat{a}}, -T^{\hat{4}}\}$. It interchanges $SU(2)_L$ and $SU(2)_R$ and flips the direction of $T^{\hat{4}}$. Accordingly P_H-odd fields are

$$P_H \text{ odd: } W_\mu^{\prime(n)}, Z_\mu^{\prime(n)}, A_\mu^{\hat{4}(n)}, H^{(n)}, D_-^{a(n)}. \tag{3.9}$$

Other fields are P_H-even.

As for the fermions, a consistent model is obtained with the bulk mass parameters $c_1 = c_2 \equiv c_q$ and $c_3 = c_4 \equiv c_\ell$. Let us first consider the multiplets containing quarks, namely, Ψ_1 and Ψ_2 in (2.7) and $\hat{\chi}^q_{1R}$, $\hat{\chi}^q_{2R}$, $\hat{\chi}^q_{3R}$, in (2.9). They are classified in terms of electric charge $Q_E = \frac{5}{3}, \frac{2}{3}, -\frac{1}{3}, -\frac{4}{3}$.

We recall that components of $\check{\Psi}$ in (2.7) are related to the components Ψ^k ($k = 1 \sim 5$) in the vectorial representation by

$$\begin{aligned}
\check{\Psi} &= \begin{pmatrix} \check{\Psi}_{11} & \check{\Psi}_{12} \\ \check{\Psi}_{21} & \check{\Psi}_{22} \end{pmatrix}\\
&= -\frac{1}{\sqrt{2}}\begin{pmatrix} \Psi^2 + i\Psi^1 & -\Psi^4 - i\Psi^3 \\ \Psi^4 - i\Psi^3 & \Psi^2 - i\Psi^1 \end{pmatrix}.
\end{aligned} \tag{3.10}$$

Ψ^4 and Ψ^5 couple with $A_z^{\hat{4}}$ or θ_H. Conversely we have, for the third generation in the twisted gauge,

$$\begin{pmatrix}\tilde{\Psi}_1^1\\ \tilde{\Psi}_1^2\\ \tilde{\Psi}_1^3\\ \tilde{\Psi}_1^4\\ \tilde{\Psi}_1^5\end{pmatrix}=\begin{pmatrix}i(\tilde{T}-\tilde{b})/\sqrt{2}\\ -(\tilde{T}+\tilde{b})/\sqrt{2}\\ -i(\tilde{B}+\tilde{t})/\sqrt{2}\\ -(\tilde{B}-\tilde{t})/\sqrt{2}\\ t'\end{pmatrix},\quad \begin{pmatrix}\tilde{\Psi}_2^1\\ \tilde{\Psi}_2^2\\ \tilde{\Psi}_2^3\\ \tilde{\Psi}_2^4\\ \tilde{\Psi}_2^5\end{pmatrix}=\begin{pmatrix}i(\tilde{U}-\tilde{Y})/\sqrt{2}\\ -(\tilde{U}+\tilde{Y})/\sqrt{2}\\ -i(\tilde{D}+\tilde{X})/\sqrt{2}\\ -(\tilde{D}-\tilde{X})/\sqrt{2}\\ b'\end{pmatrix}. \tag{3.11}$$

Ω_H transformation gives $(\tilde{\Psi}^1,\tilde{\Psi}^2,\tilde{\Psi}^3,\tilde{\Psi}^4,\tilde{\Psi}^5)\to(\tilde{\Psi}^1,\tilde{\Psi}^2,\tilde{\Psi}^3,-\tilde{\Psi}^4,\tilde{\Psi}^5)$. The $\tilde{\Psi}^4$ component is P_H-odd, whereas other components are P_H-even.

The $Q_E=\frac{5}{3}$ sector consists of T in Ψ_1 and $\hat{T}_R$ in $\hat{\chi}^q_{1R}$. The $Q_E=-\frac{4}{3}$ sector consists of Y in Ψ_2 and $\hat{Y}_R$ in $\hat{\chi}^q_{3R}$. There are no light modes in these two sectors.

The $Q_E=\frac{2}{3}$ sector consists of B, t, t' in Ψ_1, U in Ψ_2, $\hat{B}_R$ in $\hat{\chi}^q_{1R}$, and $\hat{U}_R$ in $\hat{\chi}^q_{2R}$. The bulk fermions have the following Kaluza-Klein expansion:

$$\begin{aligned}
\begin{pmatrix}\tilde{U}_L\\ (\tilde{B}_L+\tilde{t}_L)/\sqrt{2}\\ \tilde{t}'_L\end{pmatrix}(x,z)&=\sqrt{k}\sum_{n=0}^{\infty}\begin{pmatrix}a_U^{(n)}C_L(z;\lambda_n,c_t)\\ a_{B+t}^{(n)}C_L(z;\lambda_n,c_t)\\ a_{t'}^{(n)}S_L(z;\lambda_n,c_t)\end{pmatrix}\psi^{(n)}_{(2/3)(+),L}(x),\\
\begin{pmatrix}\tilde{U}_R\\ (\tilde{B}_R+\tilde{t}_R)/\sqrt{2}\\ \tilde{t}'_R\end{pmatrix}(x,z)&=\sqrt{k}\sum_{n=0}^{\infty}\begin{pmatrix}a_U^{(n)}S_R(z;\lambda_n,c_t)\\ a_{B+t}^{(n)}S_R(z;\lambda_n,c_t)\\ a_{t'}^{(n)}C_R(z;\lambda_n,c_t)\end{pmatrix}\psi^{(n)}_{(2/3)(+),R}(x),\\
\begin{pmatrix}(\tilde{B}_L-\tilde{t}_L)/\sqrt{2}\\ (\tilde{B}_R-\tilde{t}_R)/\sqrt{2}\end{pmatrix}(x,z)&=\sqrt{k}\sum_{n=1}^{\infty}a_{B-t}^{(n)}\begin{pmatrix}C_L(z;\lambda_n,c_t)t^{(n)}_{(-),L}(x)\\ S_R(z;\lambda_n,c_t)t^{(n)}_{(-),R}(x)\end{pmatrix}.
\end{aligned} \tag{3.12}$$

Here c_t is the bulk kink mass for the third generation (Ψ_1,Ψ_2), and

$$\begin{aligned}
\begin{pmatrix}C_L\\ S_L\end{pmatrix}(z;\lambda,c)&=\pm\frac{\pi}{2}\lambda\sqrt{zz_L}F_{c+(1/2),c\mp(1/2)}(\lambda z,\lambda z_L),\\
\begin{pmatrix}C_R\\ S_R\end{pmatrix}(z;\lambda,c)&=\mp\frac{\pi}{2}\lambda\sqrt{zz_L}F_{c-(1/2),c\pm(1/2)}(\lambda z,\lambda z_L).
\end{aligned} \tag{3.13}$$

$\psi^{(n)}_{(2/3)(+)}(x)$ fields are P_H-even, while $t^{(n)}_{(-)}(x)$ fields are P_H-odd. $\{\psi^{(n)}_{(2/3)(+)}(x)\}$ contains three KK towers, including the KK tower $t^{(n)}_{(+)}(x)$ of the top quark. The brane fields $\hat{B}_R$ and $\hat{U}_R$ can be expressed in terms of the bulk fields.

The spectrum λ_n and mode coefficients $a^{(n)}$ of the P_H-even towers satisfy

$$\det\hat{K}=0,\qquad \hat{K}\begin{pmatrix}a_U^{(n)}\\ \frac{1}{2}a_{B+t}^{(n)}\\ \frac{1}{\sqrt{2}}a_{t'}^{(n)}\end{pmatrix}=0, \tag{3.14}$$

where

$$\hat{K}=\begin{pmatrix}\lambda_nS_R-\frac{\mu_2^2}{2k}C_L & -\frac{\mu_2\tilde{\mu}}{2k}C_L & \frac{\mu_2\tilde{\mu}}{2k}S_L\\ 0 & \lambda_nS_R-\frac{\mu_1^2}{2k}C_L & \left(\lambda_nC_R-\frac{\mu_1^2}{2k}S_L\right)\\ -\frac{\mu_2\tilde{\mu}}{2k}C_L & \lambda_nS_R-\frac{\tilde{\mu}^2}{2k}C_L & -\left(\lambda_nC_R-\frac{\tilde{\mu}^2}{2k}S_L\right)\end{pmatrix},$$
$$C_{L,R}=C_{L,R}(1;\lambda_n,c_t),\quad S_{L,R}=S_{L,R}(1;\lambda_n,c_t). \tag{3.15}$$

Here we have suppressed a superscript q in μ_j^q. There is one light mode (the top quark) with $m_t=k\lambda_{t,0}\ll m_{\rm KK}$. When $\mu_j^2,\tilde{\mu}^2\gg m_{\rm KK}$, the spectrum of the top quark tower satisfies

$$2\left(1+\frac{\tilde{\mu}^2}{\mu_2^2}\right)S_R(1;\lambda_{t,n},c_t)S_L(1;\lambda_{t,n},c_t)+1=0 \tag{3.16}$$

for $k\lambda_{t,n}\ll m_{\rm KK}$. A similar relation is obtained for the bottom quark $m_b=k\lambda_{b,0}$:

$$2\left(1+\frac{\mu_2^2}{\tilde{\mu}^2}\right)S_R(1;\lambda_{b,n},c_t)S_L(1;\lambda_{b,n},c_t)+1=0 \tag{3.17}$$

for $k\lambda_{b,n}\ll m_{\rm KK}$. With (m_t,m_b) given, Eqs. (3.16) and (3.17) determine the bulk mass c_t and the ratio $\tilde{\mu}^2/\mu_2^2$. We note that $\tilde{\mu}^2/\mu_2^2\sim m_b/m_t$ for $m_b\ll m_t$. The spectrum of the KK tower $t^{(n)}_{(-)}(x)$ is determined by $C_L(1;\lambda_n,c_t)=0$.

Parallel arguments apply to the $Q_E=-\frac{1}{3}$ sector, which consists of b in Ψ_1, D, X, b' in Ψ_2, $\hat{D}_R$ in $\hat{\chi}^q_{2R}$, and $\hat{X}_R$ in $\hat{\chi}^q_{3R}$. The bulk fields are expanded as

$$\begin{pmatrix} \tilde{b}_L \\ (\tilde{D}_L + \tilde{X}_L)/\sqrt{2} \\ \tilde{b}'_L \end{pmatrix}(x,z) = \sqrt{k}\sum_{n=0}^{\infty}\begin{pmatrix} a_b^{(n)} C_L(z;\lambda_n,c_t) \\ a_{D+X}^{(n)} C_L(z;\lambda_n,c_t) \\ a_{b'}^{(n)} S_L(z;\lambda_n,c_t) \end{pmatrix}\psi^{(n)}_{-(1/3)(+),L}(x),$$

$$\begin{pmatrix} \tilde{b}_R \\ (\tilde{D}_R + \tilde{X}_R)/\sqrt{2} \\ \tilde{b}'_R \end{pmatrix}(x,z) = \sqrt{k}\sum_{n=0}^{\infty}\begin{pmatrix} a_b^{(n)} S_R(z;\lambda_n,c_t) \\ a_{D+X}^{(n)} S_R(z;\lambda_n,c_t) \\ a_{b'}^{(n)} C_R(z;\lambda_n,c_t) \end{pmatrix}\psi^{(n)}_{-(1/3)(+),R}(x), \tag{3.18}$$

$$\begin{pmatrix} (\tilde{D}_L - \tilde{X}_L)/\sqrt{2} \\ (\tilde{D}_R - \tilde{X}_R)/\sqrt{2} \end{pmatrix}(x,z) = \sqrt{k}\sum_{n=1}^{\infty} a_{D-X}^{(n)}\begin{pmatrix} C_L(z;\lambda_n,c_t) b^{(n)}_{(-),L}(x) \\ S_R(z;\lambda_n,c_t) b^{(n)}_{(-),R}(x) \end{pmatrix}.$$

The equations and relations in the $Q_E = -\frac{1}{3}$ sector are obtained from those in the $Q_E = \frac{2}{3}$ sector by replacing (U, B, t, t') and $(\mu_1, \mu_2, \tilde{\mu})$ by (b, D, X, b') and $(\mu_3, \tilde{\mu}, \mu_2)$, respectively.

Similar relations are obtained in the lepton sector. The generation mixing is incorporated by considering μ_2, $\tilde{\mu}$ in matrices.

IV. 4D GAUGE COUPLINGS

The 4D gauge couplings are obtained by performing overlapping integrals of wave functions. Generalizing the argument in Ref. [18], one can write, for the t and b quarks and the τ and ν_τ leptons in the third generation, the couplings of the photon, W boson, Z boson, and gluon towers as

$$\begin{aligned}
&\sum_n A_\mu^{\gamma(n)}\left\{\frac{2}{3}(g_{tL}^{\gamma(n)}\bar{t}_L\gamma^\mu t_L + g_{tR}^{\gamma(n)}\bar{t}_R\gamma^\mu t_R) - \frac{1}{3}(g_{bL}^{\gamma(n)}\bar{b}_L\gamma^\mu b_L + g_{b_R}^{\gamma(n)}\bar{b}_R\gamma^\mu b_R) - (g_{\tau L}^{\gamma(n)}\bar{\tau}_L\gamma^\mu\tau_L + g_{\tau_R}^{\gamma(n)}\bar{\tau}_R\gamma^\mu\tau_R)\right\} \\
&\quad + \sum_n \frac{1}{\sqrt{2}} W_\mu^{(n)}\{g_{tb,L}^{W(n)}\bar{b}_L\gamma^\mu t_L + g_{tb,R}^{W(n)}\bar{b}_R\gamma^\mu t_R + g_{\tau,L}^{W(n)}\bar{\tau}_L\gamma^\mu\nu_{\tau L} + g_{\tau,R}^{W(n)}\bar{\tau}_R\gamma^\mu\nu_{\tau R}\} + \text{H.c.} \\
&\quad + \sum_n \frac{1}{\cos\theta_W} Z_\mu^{(n)}\{g_{tL}^{Z(n)}\bar{t}_L\gamma^\mu t_L + g_{tR}^{Z(n)}\bar{t}_R\gamma^\mu t_R + g_{bL}^{Z(n)}\bar{b}_L\gamma^\mu b_L + g_{bR}^{Z(n)}\bar{b}_R\gamma^\mu b_R + g_{\nu_\tau L}^{Z(n)}\bar{\nu}_{\tau L}\gamma^\mu\nu_{\tau L} \\
&\quad + g_{\nu_\tau R}^{Z(n)}\bar{\nu}_{\tau R}\gamma^\mu\nu_{\tau R} + g_{\tau L}^{Z(n)}\bar{\tau}_L\gamma^\mu\tau_L + g_{\tau R}^{Z(n)}\bar{\tau}_R\gamma^\mu\tau_R\} + \sum_n G_\mu^{(n)a}\left\{\left(g_{tL}^{G(n)}\bar{t}_L\gamma^\mu\frac{1}{2}\lambda^a t_L + g_{tR}^{G(n)}\bar{t}_R\gamma^\mu\frac{1}{2}\lambda^a t_R\right)\right. \\
&\quad \left. + \left(g_{bL}^{G(n)}\bar{b}_L\gamma^\mu\frac{1}{2}\lambda^a b_L + g_{b_R}^{G(n)}\bar{b}_R\gamma^\mu\frac{1}{2}\lambda^a b_R\right)\right\}.
\end{aligned} \tag{4.1}$$

From the H parity invariance the W', Z', and $A^{\hat{4}}$ gauge boson towers do not couple to the quarks and leptons.

The couplings of the photon tower with the t and b quarks and τ lepton are given, with $h^L_{\gamma^{(n)}} = h^R_{\gamma^{(n)}} = (g_B/g_A)h^B_{\gamma^{(n)}} \equiv h_{\gamma^{(n)}}(z)$, by

$$\begin{aligned}
g_{tL}^{\gamma(n)} &= g_A\int_1^{z_L} dz h_{\gamma^{(n)}}\{(a_U^2 + a_{B+t}^2)C_L(\lambda_t)^2 + a_{t'}^2 S_L(\lambda_t)^2\}, \\
g_{bL}^{\gamma(n)} &= g_A\int_1^{z_L} dz h_{\gamma^{(n)}}\{(a_b^2 + a_{D+X}^2)C_L(\lambda_b)^2 + a_{b'}^2 S_L(\lambda_b)^2\}, \\
g_{\tau L}^{\gamma(n)} &= g_A\int_1^{z_L} dz h_{\gamma^{(n)}}\{(a_{L_{3Y}}^2 + a_{\tau+L_{1X}}^2)C_L(\lambda_\tau)^2 + a_{\tau'}^2 S_L(\lambda_\tau)^2\}.
\end{aligned} \tag{4.2}$$

Here $C_L(\lambda_t) = C_L(z;\lambda_t,c_t)$ etc.. The formulas for right-handed fermions are obtained from those for the corresponding left-handed fermions by replacing C_L and S_L by S_R and C_R, respectively. The couplings of the W boson towers are given by

$$\begin{aligned}
g_{tb,L}^{W(n)} &= g_A\int_1^{z_L} dz\{2h_{W^{(n)}}(a_b a_{B+t} + a_U a_{D+X})C_L(\lambda_t)C_L(\lambda_b) \\
&\quad + \sqrt{2}h^{\wedge}_{W^{(n)}}(a_B a_{t'}C_L(\lambda_b)S_L(\lambda_t) - a_{b'}a_U S_L(\lambda_b)C_L(\lambda_t))\}, \\
g_{\tau,L}^{W(n)} &= g_A\int_1^{z_L} dz\{2h_{W^{(n)}}(a_{\nu_\tau}a_{\tau+L_{1X}} + a_{L_{3Y}}a_{L_{2Y}+L_{3X}}) \\
&\quad \times C_L(\lambda_\tau)C_L(\lambda_{\nu_\tau}) + \sqrt{2}h^{\wedge}_{W^{(n)}}(a_{L_{3Y}}a_{\nu'_\tau}C_L(\lambda_\tau)S_L(\lambda_{\nu_\tau}) \\
&\quad - a_{\tau'}a_{\nu_\tau}S_L(\lambda_{\nu_\tau})C_L(\lambda_\tau))\},
\end{aligned} \tag{4.3}$$

where $h_{W^{(n)}} \equiv h^L_{W^{(n)}} = h^R_{W^{(n)}}$. The couplings of the Z boson towers are parametrized as

$$\begin{aligned}
g_{tL,R}^{Z(n)} &= +\frac{1}{2}g_{tL,R}^{Z(n),T} - \frac{2}{3}g_{tL,R}^{Z(n),Q}\sin^2\theta_W, \\
g_{bL,R}^{Z(n)} &= -\frac{1}{2}g_{bL,R}^{Z(n),T} + \frac{1}{3}g_{bL,R}^{Z(n),Q}\sin^2\theta_W, \quad g_{\nu_\tau L,R}^{Z(n)} = +\frac{1}{2}g_{\nu_\tau L,R}^{Z(n),T}, \\
g_{\tau L,R}^{Z(n)} &= -\frac{1}{2}g_{\tau L,R}^{Z(n),T} + g_{\tau L,R}^{Z(n),Q}\sin^2\theta_W.
\end{aligned} \tag{4.4}$$

In the SM $g_{fL}^{Z,T} = g_{fL}^{Z,Q} = g_{fR}^{Z,Q} = g_w$ and $g_{fR}^{Z,T} = 0$. In the current model, with the aid of (A5), one finds that

$$
\begin{aligned}
g_{tL}^{Z^{(n)},T} &= \frac{\sqrt{2}g_A}{\sqrt{r_{Z^{(n)}}}} \int_1^{z_L} dz\{a_U^2 C_{Z^{(n)}} C_L(\lambda_t)^2 - 2a_{B+t}a_{t'}\hat{S}_{Z^{(n)}} C_L(\lambda_t)S_L(\lambda_t)\},\\
g_{bL}^{Z^{(n)},T} &= \frac{\sqrt{2}g_A}{\sqrt{r_{Z^{(n)}}}} \int_1^{z_L} dz\{a_b^2 C_{Z^{(n)}} C_L(\lambda_b)^2 + 2a_{D+X}a_{b'}\hat{S}_{Z^{(n)}} C_L(\lambda_b)S_L(\lambda_b)\},\\
g_{\nu_\tau L}^{Z^{(n)},T} &= \frac{\sqrt{2}g_A}{\sqrt{r_{Z^{(n)}}}} \int_1^{z_L} dz\{a_{\nu_\tau}^2 C_{Z^{(n)}} C_L(\lambda_{\nu_\tau})^2 - 2a_{L_{2Y}+L_{3X}}a_{\nu'_\tau}\hat{S}_{Z^{(n)}} C_L(\lambda_{\nu_\tau})S_L(\lambda_{\nu_\tau})\},\\
g_{\tau L}^{Z^{(n)},T} &= \frac{\sqrt{2}g_A}{\sqrt{r_{Z^{(n)}}}} \int_1^{z_L} dz\{a_{L_{3Y}}^2 C_{Z^{(n)}} C_L(\lambda_\tau)^2 + 2a_{\tau+L_{1X}}a_{\tau'}\hat{S}_{Z^{(n)}} C_L(\lambda_\tau)S_L(\lambda_\tau)\},\\
g_{tL}^{Z^{(n)},Q} &= \frac{\sqrt{2}g_A}{\sqrt{r_{Z^{(n)}}}} \int_1^{z_L} dz C_{Z^{(n)}}\{(a_U^2 + a_{B+t}^2)C_L(\lambda_t)^2 + a_{t'}^2 S_L(\lambda_t)^2\},\\
g_{bL}^{Z^{(n)},Q} &= \frac{\sqrt{2}g_A}{\sqrt{r_{Z^{(n)}}}} \int_1^{z_L} dz C_{Z^{(n)}}\{(a_b^2 + a_{D+X}^2)C_L(\lambda_b)^2 + a_{b'}^2 S_L(\lambda_b)^2\},\\
g_{\tau L}^{Z^{(n)},Q} &= \frac{\sqrt{2}g_A}{\sqrt{r_{Z^{(n)}}}} \int_1^{z_L} dz C_{Z^{(n)}}\{(a_{L_{3Y}}^2 + a_{\tau+L_{1X}}^2)C_L(\lambda_\tau)^2 + a_{\tau'}^2 S_L(\lambda_\tau)^2\},
\end{aligned}
\tag{4.5}
$$

where $C_{Z^{(n)}} = C(z;\lambda_{Z^{(n)}})$, etc.

The couplings of the gluon towers $g_{tI}^{G^{(n)}}$ and $g_{bI}^{G^{(n)}}$ are obtained from the photon tower couplings $g_{tI}^{\gamma^{(n)}}$ and $g_{bI}^{\gamma^{(n)}}$ with the replacement of the five-dimensional coupling, $g_{tI}^{G^{(n)}} = (g_C/g_A)g_{tI}^{\gamma^{(n)}}$ and $g_{bI}^{G^{(n)}} = (g_C/g_A)g_{bI}^{\gamma^{(n)}}$. The photon and gluon couplings are universal, that is, $e = g_{tI}^{\gamma^{(0)}} = g_{bI}^{\gamma^{(0)}} = (g_A/\sqrt{L})\sin\theta_W$. The other couplings exhibit violation of the universality as evaluated below.

A. Zero mode couplings

The numerical values for the various gauge couplings are obtained with the input parameters given in Sec. II. The couplings of the W boson with quarks and leptons are tabulated in Table II. The ratios of the couplings to the 4D $SU(2)$ coupling, $g_f^{(W)}\sqrt{L}/g_A$, have been tabulated. Except for tb, the couplings are almost universal. For the $t_L b_L$ coupling the deviation amounts to 2%–6% for $z_L = 10^{15} \sim 10^5$. The $t_R b_R$ coupling is about 0.09%–0.3% of the left-handed coupling for $z_L = 10^{15} \sim 10^5$.

The couplings of the Z boson with quarks are tabulated in Table III. For reference, the tree-level values in the standard model, $1/2 - (2/3)\sin^2\theta_W$ and $-1/2 + (1/3)\sin^2\theta_W$ for left-handed quarks and $-(2/3)\sin^2\theta_W$

TABLE III. The couplings of Z boson with quarks, $g_f^{(Z)}\sqrt{L}/g_A$.

z_L	u_L	c_L	t_L	d_L	s_L	b_L
10^{15}	0.3485	0.3485	0.3219	−0.4260	−0.4260	−0.4265
10^{10}	0.3501	0.3501	0.3086	−0.4276	−0.4276	−0.4288
10^5	0.3548	0.3548	0.2558	−0.4325	−0.4325	−0.4369
SM		0.3459			−0.4229	

z_L	u_R	c_R	t_R	d_R	s_R	b_R
10^{15}	−0.1562	−0.1562	−0.1835	0.07811	0.07809	0.07806
10^{10}	−0.1570	−0.1570	−0.2002	0.07852	0.07847	0.07839
10^5	−0.1595	−0.1593	−0.2656	0.07976	0.07965	0.07928
SM	−0.1541			0.07707		

TABLE II. The couplings of W boson with quarks and leptons, $g_f^{(W)}\sqrt{L}/g_A$.

z_L	$u_L d_L$	$c_L s_L$	$t_L b_L$	$\nu_{eL} e_L$	$\nu_{\mu L}\mu_L$	$\nu_{\tau L}\tau_L$
10^{15}	1.0053	1.0053	0.9816	1.0053	1.0053	1.0053
10^{10}	1.0079	1.0079	0.9730	1.0079	1.0079	1.0079
10^5	1.0154	1.0154	0.9470	1.0154	1.0154	1.0153

z_L	$u_R d_R$	$c_R s_R$	$t_R b_R$	$\nu_{eR} e_R$	$\nu_{\mu R}\mu_R$	$\nu_{\tau R}\tau_R$
10^{15}	-5×10^{-12}	-5×10^{-8}	−0.0009	-3×10^{-22}	-4×10^{-16}	-6×10^{-17}
10^{10}	-6×10^{-12}	-7×10^{-8}	−0.0014	-4×10^{-22}	-7×10^{-16}	-2×10^{-13}
10^5	-9×10^{-12}	-1×10^{-7}	−0.0031	-5×10^{-22}	-1×10^{-18}	-2×10^{-16}

TABLE IV. The couplings of Z bosons with leptons, $g_f^{(Z)}\sqrt{L}/g_A$.

z_L	e_L	μ_L	τ_L	e_R	μ_R	τ_R
10^{15}	−0.2710	−0.2710	−0.2710	0.2344	0.2343	0.2343
10^{10}	−0.2725	−0.2725	−0.2725	0.2356	0.2355	0.2354
10^{5}	−0.2771	−0.2771	−0.2771	0.2394	0.2391	0.2389
SM		−0.2688			0.2312	

z_L	ν_{eL}	$\nu_{\mu L}$	$\nu_{\tau L}$	ν_{eR}	$\nu_{\mu R}$	$\nu_{\tau R}$
10^{15}	0.5035	0.5035	0.5035	-1.4×10^{-13}	-7.2×10^{-9}	-2.3×10^{-6}
10^{10}	0.5052	0.5052	0.5052	-1.8×10^{-13}	-9.7×10^{-9}	-3.2×10^{-6}
10^{5}	0.5102	0.5102	0.5101	-2.5×10^{-13}	-1.5×10^{-8}	-5.4×10^{-6}
SM		0.5			0	

TABLE V. χ^2 fit for A_{FB} and Z decay fractions. The values of $m_{\rm KK}$, m_H, and $m_W^{\rm tree}$ (W mass at the tree level) are also listed.

	Number of data	$z_L = 10^{15}$	10^{10}	10^{5}	SM
$\sin^2\theta_W$		0.2309	0.2303	0.2284	0.2312
χ^2 [A_{FB}]	6	6.3	6.4	7.1	10.8
χ^2 [Z decay fractions]	8	16.5	37.7	184.5	13.6
Sum of two χ^2	14	22.8	44.1	191.6	24.5
$m_{\rm KK}$ (GeV)		1466	1193	836	
m_H (GeV)		135	108	72	
$m_W^{\rm tree}$ (GeV)		79.84	79.80	79.71	79.95

and $(1/3)\sin^2\theta_W$ for right-handed quarks, are also listed. As we shall see below, the small violation of the universality gives a better fit to the forward-backward asymmetry data. As a general character for left-handed and right-handed quarks, it is found that the coupling of right-handed quarks for a small warp factor tends to deviate from the standard model values.

The couplings of Z bosons with leptons are tabulated in Table IV. They are not very sensitive to the generation. As a general tendency, the couplings deviate more from those in the standard model as the warp factor becomes smaller.

In the standard model the couplings of the Z boson with fermions are described by the weak coupling and their quantum number, namely, by $(g_w/\cos\theta_W)(T^3 - Q\sin^2\theta_W)$, at the tree level. In the present model they have an analogous form given by $(1/\cos\theta_W)\times(g_{T,L}T^3 - g_{Q,L}Q\sin^2\theta_W)$ for left-handed fermions and by $(1/\cos\theta_W)(g_{T,R} - g_{Q,R}Q\sin^2\theta_W)$ for right-handed fermions. Here g_T and g_Q depend on the flavor of fermions. It is found that $g_{T,L} \approx g_{Q,L}$. For right-handed fermions the absolute value of $g_{T,R}\sqrt{L}/g_A$ is small for the t quark ($\lesssim 10^{-2}$) and very small for the others ($\lesssim 10^{-6}$), but $g_{Q,R}\sqrt{L}/g_A$ can be of order $\mathcal{O}(1)$ which leads to deviation from the standard model. The couplings of the Z boson with right-handed neutrinos are very small as neutral fields have only the g_T component. For a similar reason the couplings of the KK Z boson with right-handed neutrinos turn out to be very small.

B. Forward-backward asymmetry

The forward-backward asymmetry on the Z resonance is given by

$$A_{FB}^f = \frac{3}{4}\left[\frac{(g_{eL}^Z)^2 - (g_{eR}^Z)^2}{(g_{eL}^Z)^2 + (g_{eR}^Z)^2}\right]\left[\frac{(g_{fL}^Z)^2 - (g_{fR}^Z)^2}{(g_{fL}^Z)^2 + (g_{fR}^Z)^2}\right], \quad (4.6)$$

which is evaluated from the gauge couplings given in the preceding subsection. A_{FB}^f does not depend on the absolute common magnitude of g_A, but sensitively depends on $\sin^2\theta_W$. The branching fractions of various decay modes of the Z boson also sensitively depend on $\sin^2\theta_W$. We have determined the value of $\sin^2\theta_W$ to minimize χ^2 of those experimental data as tabulated in Table V. The value of $\sin^2\theta_W$ turns out a bit smaller than that in the standard model.

With given $\sin^2\theta_W$ the numerical values of A_{FB}^f are shown in Table VI.[1] The experimental values are quoted from Ref. [50]. The current model gives a rather good fit for the forward-backward asymmetries A_{FB}^f, though the fit to the Z decay fractions becomes poor for smaller values of z_L.

[1]The result for $z_L = 10^{15}$ has been given in Ref. [43]. A slight difference in the numerical values is due to the different choice of the values of the input parameters.

TABLE VI. The forward-backward asymmetry on the Z resonance, A_{FB}^{f}.

	Experiments	$z_L = 10^{15}$	$z_L = 10^{10}$	$z_L = 10^5$	SM
e	0.0145 ± 0.0025	0.0156	0.0157	0.0159	$0.016\,33 \pm 0.000\,21$
μ	0.0169 ± 0.0013	0.0156	0.0157	0.0160	
τ	0.0188 ± 0.0017	0.0156	0.0158	0.0161	
s	0.0976 ± 0.0114	0.1011	0.1014	0.1019	0.1035 ± 0.0007
c	0.0707 ± 0.0035	0.0720	0.0721	0.0725	0.0739 ± 0.0005
b	0.0992 ± 0.0016	0.1011	0.1014	0.1021	0.1034 ± 0.0007

C. Decay width

The partial decay width of the Z boson is given by

$$\Gamma(Z \to f\bar{f}) = \frac{m_Z}{12\pi\cos^2\theta_W} F(g_{fL}^{(Z)}, g_{fR}^{(Z)}, m_f, m_Z),$$
$$F(g_{fL}, g_{fR}, m_f, m_V) = \left\{\frac{(g_{fL})^2 + (g_{fR})^2}{2} + 2g_{fL}g_{fR}\frac{m_f^2}{m_V^2}\right\}\sqrt{1 - \frac{4m_f^2}{m_V^2}}. \quad (4.7)$$

Here the couplings $g_{fL}^{(Z)}$ and $g_{fR}^{(Z)}$ are given in Tables III and IV. For quarks the formula should be multiplied by a factor $3(1 + \alpha_s/\pi)$.

For $z_L = 10^{15}$, 10^{10}, 10^5, the branching fractions in Z decay are shown in Table VII. The experimental values are quoted from Ref. [50]. The tree-level prediction for branching fractions reproduces the pattern of the experimental values well for $z_L = 10^{15}$.

The total decay width $\Gamma_{\rm tot}$ depends on $\alpha(m_Z)$. The value of $\alpha(m_Z)$ determined to fit the experimental value $\Gamma_{\rm tot}$ does not agree well with the value determined by the renormalization group from the low energy data. For $z_L = 10^{15}$, for instance, one finds $\alpha^{-1}(m_Z) = 130.5$. At the moment one cannot reliably evaluate one-loop corrections to $\Gamma_{\rm tot}$ in the gauge-Higgs unification scenario and this mismatch is understood within that error.

TABLE VII. The branching fractions in the Z boson decay. The invisible decay in the model means the decay into $\nu_e + \nu_\mu + \nu_\tau$.

z_L	10^{15}	10^{10}	10^5	Experiments
$e(\%)$	3.374	3.382	3.403	3.363 ± 0.004
$\mu(\%)$	3.373	3.380	3.400	3.366 ± 0.007
$\tau(\%)$	3.368	3.374	3.392	3.370 ± 0.008
Invisible (%)	19.99	19.95	19.82	20.00 ± 0.06
$(u + c)/2(\%)$	11.93	11.94	11.95	11.6 ± 0.6
$(d + s + b)/3(\%)$	15.34	15.34	15.36	15.6 ± 0.4
$c(\%)$	11.93	11.94	11.95	12.03 ± 0.21
$b(\%)$	15.34	15.37	15.53	15.21 ± 0.05

V. PRODUCTION OF HIGGS BOSONS AT COLLIDERS

The mass of the Higgs boson is in the range 70–140 GeV, depending on the warp factor z_L. Higgs bosons can be copiously produced at colliders at high energies. At $\theta_H = \frac{1}{2}\pi$, however, there emerges the H parity conservation so that Higgs bosons can be produced only in pairs, provided no other KK modes of P_H-odd fields are produced. Furthermore, the Higgs boson becomes stable at $\theta_H = \frac{1}{2}\pi$ so that conventional ways of detecting the Higgs boson, namely, of finding decay products of the Higgs boson, turn out fruitless. In the current scheme the produced Higgs boson appears as missing energy and momentum. At colliders there appear at least two particles of missing energy and momentum, which makes detection hard. There is a large background containing neutrinos.

An interesting feature of the present model is that the stable Higgs boson is much lighter than the KK particles, that is, $m_H \ll m_{KK}$ as seen in Table V. Hence it is natural to investigate the Higgs production with the effective Lagrangian among low energy fields (W, Z, quarks, and leptons) at $\theta_H = \frac{1}{2}\pi$ [19,39],

$$\mathcal{L}_{\rm eff} \sim -\left\{m_W^2 W_\mu^\dagger W^\mu + \frac{1}{2}m_Z^2 Z_\mu Z^\mu\right\}\cos^2\frac{H}{f_H} - \sum_a m_a \bar{\psi}_a \psi_a \cos\frac{H}{f_H}. \quad (5.1)$$

Here $f_H \sim 246$ GeV. The form of (5.1) is valid only when the relevant energy scale is sufficiently smaller than $m_{\rm KK}$. For the pair production of Higgs bosons (5.1) leads to

$$\mathcal{L}_{\rm eff} \sim \sum_a \frac{m_a}{2f_H^2} H^2 \bar{\psi}_a \psi_a + \frac{m_W^2}{f_H^2} H^2 W_\mu^\dagger W^\mu + \frac{m_Z^2}{2f_H^2} H^2 Z_\mu Z^\mu. \quad (5.2)$$

The sign of the $H^2W^\dagger W$ and H^2ZZ couplings is opposite to that in the SM [36]. Collider signatures of Higgs bosons in the current model have been previously investigated with this effective Lagrangian by Cheung and Song[21] and by Alves [22].

A. Pair production of Higgs bosons at LHC

Pair production processes of Higgs bosons at LHC have been studied in Refs. [21,22]. Cheung and Song evaluated the cross section of the Higgs pair production associated with a W or Z boson and found that the $ZHH(WHH)$ cross section is 0.2(0.4) fb for the case that $m_H = 70$ GeV and the missing transverse momentum $\not{p}_T$ is larger than 100 GeV. On the other hand the cross section of the background process $ZZ \to Z\nu\bar{\nu}$ ($WZ \to W\nu\bar{\nu}$) was estimated as 370(390) fb. Thus positive identification of either of the signals is virtually impossible assuming an integrated luminosity of 100 fb^{-1}.

Alves studied the Higgs pair production in the weak boson fusion (WBF), in which the signal is a pair of forward and backward jets and a missing transverse momentum. This signal is quite similar to that of the single production of the Higgs boson decaying invisibly [52]. In Ref. [22], the signal cross section at 14 TeV LHC is estimated as 4.05(4.03) fb for $m_H = 70(90)$ GeV using the same set of cuts employed in Ref. [52]. The background cross section is the same as that in Ref. [52] and amounts to 167 fb. Alves concluded that 255(257) fb^{-1} is required for a 5σ discovery.

Here we present a brief estimate of the cross section of the Higgs pair production by the WBF in the present model by relating it to the single Higgs production by the WBF in the SM. Inspecting the relevant Feynman rules in the present model and the SM, we find that $f_H^2|\mathcal{M}(HH)|^2 = |\mathcal{M}(h)|^2_{m_h^2=m_{HH}^2}$, where h represents the Higgs boson in the SM, $\mathcal{M}(HH)$ [$\mathcal{M}(h)$] denotes the amplitude of the double (single) Higgs production by the WBF process in the present model (SM), m_h is the Higgs boson mass in the SM, and m_{HH} is the invariant mass of the pair of Higgs bosons in the present model. Taking the two-body phase space of the Higgs pair and the statistical factor due to the existence of identical particles into account, we obtain the following relation,

$$\frac{d\sigma(HH)}{dm_{HH}^2} = \frac{1}{32\pi^2 f_H^2}\sqrt{1-\frac{4m_H^2}{m_{HH}^2}}\,\sigma(h)|_{m_h^2=m_{HH}^2}, \qquad (5.3)$$

where $\sigma(HH)$ [$\sigma(h)$] represents the cross section of the double (single) Higgs production by the WBF in the present model (SM).

The total cross section is evaluated by integrating Eq. (5.3) over m_{HH}^2 in the kinematically allowed interval. The upper value of the integration region could be as large as the center-of-mass energy squared of pp collisions in principle. However, as mentioned above, the effective Lagrangian in Eq. (5.2) is applicable in a limited energy scale. We choose $4m_{KK}^2$ as the upper value for an illustration. We note that $4m_{KK}^2 \simeq (1.7\ \text{TeV})^2$ for the case that $z_L = 10^5$ is approximately the same as the unitarity bound of 1.8 TeV obtained in Ref. [22]. We evaluate the right-hand side of Eq. (5.3) at the parton level with the CTEQ6L parton distribution function [53] and the cuts used in Refs. [22,52]. Our numerical calculation is done by MADGRAPH/MADEVENT [54] without hadronization or detector simulation.

The signal cross section at 14 TeV LHC is approximately 1.3 fb for $z_L = 10^5$–10^{15}. Our result is smaller by about a factor of 3 than that of Ref. [22]. Thus, an integrated luminosity of a few ab^{-1} seems to be required to observe the signal.

B. Pair production of Higgs bosons at ILC

Cheung and Song have studied the Higgs pair production process $e^-e^+ \to ZHH$ at ILC along with the background process $e^-e^+ \to Z\nu\bar{\nu}$. The Feynman diagram of the signal process is depicted in Fig. 1. The integrated luminosity for a 5σ discovery seems to be larger than several ab^{-1} at 500 GeV ILC according to their result.

The differential cross section of $e_R^- e_L^+ \to Z_T HH$, where Z_T denotes the transversely polarized Z boson, is given by

$$\frac{d\sigma_{RL}^T}{dx\,d\cos\theta} = \frac{g_R^2 m_Z^4 s}{2(4\pi)^3 f_H^4 (s-m_Z^2)^2} \times \sqrt{\frac{(x_{\max}-x)(x^2-x_{\min}^2)}{1+x_{\min}^2/4-x}}\,\frac{1+\cos^2\theta}{2}. \qquad (5.4)$$

Here g_R denotes the coupling constant of the right-handed electron to the Z boson, which is given by $g_R|_{\text{SM}} = -\sqrt{g^2+g'^2}\sin^2\theta_W$ in the standard model, and θ is the angle between the momentum of the electron and that of the Z boson in the center-of-mass system. The energy of the Z boson normalized to the beam energy, x, and its minimal and maximal values are given by

$$x = \frac{E_Z}{\sqrt{s}/2}, \qquad x_{\min} = \frac{m_Z}{\sqrt{s}/2}, \qquad x_{\max} = 1 - \frac{4m_H^2}{s} + \frac{x_{\min}^2}{4}. \qquad (5.5)$$

For $e_R^- e_L^+ \to Z_L HH$, where Z_L denotes the longitudinal Z boson, the differential cross section is given by

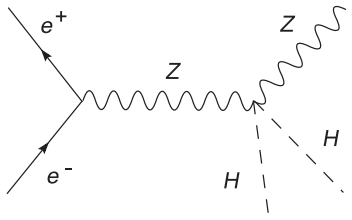

FIG. 1. Pair production of Higgs bosons at ILC.

$$\frac{d\sigma_{RL}^{L}}{dx\,d\cos\theta} = \frac{g_R^2 m_Z^4 s}{2(4\pi)^3 f_H^4 (s-m_Z^2)^2} \times \sqrt{\frac{(x_{\max}-x)(x^2-x_{\min}^2)}{1+x_{\min}^2/4-x}}\,\frac{x^2}{x_{\min}^2}\,\frac{1-\cos^2\theta}{2}. \tag{5.6}$$

For the case of $e_L^- e_R^+$, g_R should be replaced by g_L in the above formulas. In the standard model $g_L|_{\rm SM} = \sqrt{g^2+g'^2}(1/2-\sin^2\theta_W)$.

Figure 2 shows the total cross sections of $e^-e^+ \to Z_T HH$ and $e^-e^+ \to Z_L HH$ and their sum as functions of $\sqrt{s}$ for $z_L = 10^5$. As $\sqrt{s}$ increases, the cross section of the Z_L mode asymptotically becomes constant, violating the unitarity bound. This is expected because the low energy effective Lagrangian in Eq. (5.1) does not contain vertices with an odd number of Higgs fields after integrating out all heavy KK modes. With adding diagrams with such vertices to the one in Fig. 1, the leading terms in the amplitudes cancel among each other in the standard model so that the unitarity is maintained. In the present model the KK modes appearing as internal lines of the relevant diagrams are supposed to rescue the unitarity. Put differently, the effective Lagrangian is applicable only for the case that contributions of the KK modes are negligible, that is, when $\sqrt{s} \ll m_{KK}$. Accordingly, unless otherwise stated, we take $\sqrt{s} = 500$ GeV in the following numerical calculation in this subsection.

The major background is $e^-e^+ \to Z\nu_\alpha\bar{\nu}_\alpha$ ($\alpha = e, \mu, \tau$). Their total cross section is about 300 fb for $M_{\rm mis} \geq 120$ GeV, where $M_{\rm mis}$ is the invariant mass of the neutrino pair. The background is dominated by the electron neutrino mode due to the t-channel W boson exchange. In order to reduce this large background, one may use beam polarizations. We consider the limiting case of the purely right-handed electron and the purely left-handed positron as an ideal case. As well as the beam polarizations, the missing mass cut reduces the background. Corresponding to $m_H = 72, 108, 135$ GeV for $z_L = 10^5, 10^{10}, 10^{15}$, respectively, we take $M_{\rm mis} > 120, 200, 250$ GeV. We employ the GRACE system version 2 [55] in our numerical estimation of the background.

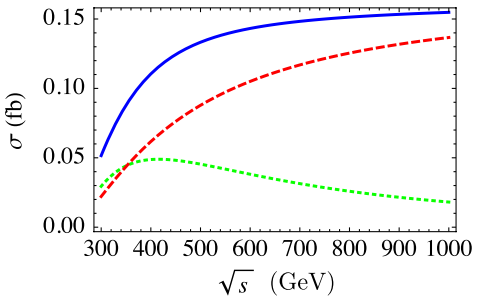

FIG. 2 (color online). Cross sections of Higgs pair production at ILC for $z_L = 10^5$. The dotted (green) line shows the Z_T mode, the dashed (red) line is the Z_L mode, and the solid (blue) represents their sum.

The statistical signification of the signal is defined by

$$S = \frac{N_{\rm signal}}{\sqrt{N_{\rm signal}+N_{\rm BG}}}, \tag{5.7}$$

where $N_{\rm signal}$ and $N_{\rm BG}$ are the expected numbers of signal and background events, respectively. They are given as $N_{\rm signal(BG)} = L\sigma_{\rm signal(BG)}B_{\rm ev}$, where L is the integrated luminosity and $B_{\rm ev} = 1 - B_{\rm invisible} - B_{\tau\bar{\tau}} = 1 - 0.200 - 0.037 = 0.763$ is the effective visible branching ratio of the Z boson. The significance of the Z_L mode turns out to be much larger than that of the Z_T mode and we concentrate on the former in order to evaluate the lower bound of integrated luminosity to establish the signal. Employing $|\cos\theta| < 0.6$, which approximately maximizes the significance, we obtain the significance of $e_R^- e_L^+ \to Z_L HH$ as $S/\sqrt{L} = 0.14, 0.073, 0.034$ for $z_L = 10^5, 10^{10}, 10^{15}$, respectively, where L is in the fb^{-1} unit. Thus, in order for 5σ, we need at least 1.3, 4.7, 21 ab^{-1} for $z_L = 10^5, 10^{10}, 10^{15}$, respectively. Since the KK mass scale is rather high as $m_{KK} = 1466$ GeV in the case of $z_L = 10^{15}$, one can apply the effective Lagrangian to a higher energy. For instance, we obtain $S/\sqrt{L} = 0.11$ for $\sqrt{s} = 750$ GeV, and the required luminosity is $L > 2.0$ ab^{-1}.

VI. SPECTRUM OF KK STATES

One of the direct ways to see the extra dimension is to produce KK excited modes of various particles and observe their decays. In the current model the H parity is conserved so that P_H-odd KK modes can be produced in a pair. Production of a single KK mode occurs only for P_H-even modes. In this section we determine spectra of various KK modes.

A. KK gauge bosons

The spectrum of KK gluons $G^{(n)}$ is identical to the spectrum of KK photons $A^{\gamma(n)}$. They are determined by the fourth equation in Eq. (3.6). The masses of KK W and Z bosons, $W^{(n)}$ and $Z^{(n)}$, are determined by the first and second equations in Eq. (3.6), whereas those of $W^{\prime(n)}$, $Z^{\prime(n)}$, and $A^{\hat{4}(n)}$ are determined by the third and fifth equations. The numerical values of the masses of the first five KK modes are given in Table VIII.

We observe that among P_H-even modes

$$\begin{aligned} m_{Z^{(1)}} &< m_{W^{(1)}} < m_{G^{(1)}} < m_{W^{(2)}} < m_{Z^{(2)}} < m_{Z^{(3)}} < m_{W^{(3)}} \\ &< m_{G^{(2)}} < m_{W^{(4)}} < m_{Z^{(4)}} < m_{Z^{(5)}} < m_{W^{(5)}} < m_{G^{(3)}} \\ &< m_{W^{(6)}} < m_{Z^{(6)}} < \cdots \end{aligned} \tag{6.1}$$

irrespective of z_L. The lighter the $n = 0$ mode is, the $n = 1$ mode becomes heavier. Masses of P_H-odd gauge bosons obey the pattern $m_{W^{\prime(n)}} = m_{Z^{\prime(n)}} \sim m_{A^{\gamma(n)}}$ and $m_{A^{\hat{4}(n)}} \sim m_{W^{(2n)}}$.

TABLE VIII. Mass spectra of KK gauge bosons in units of GeV.

	$A^{\gamma(n)}$, $G^{(n)}$				
$z_L \backslash n$	1	2	3	4	5
10^{15}	1144	2598	4061	5522	6991
10^{10}	940	2125	3316	4508	5701
10^{5}	678	1511	2347	3184	4021
	$W^{(n)}$				
$z_L \backslash n$	1	2	3	4	5
10^{15}	1133	1800	2587	3285	4050
10^{10}	927	1470	2111	2679	3301
10^{5}	659	1041	1490	1889	2325
	$Z^{(n)}$				
$z_L \backslash n$	1	2	3	4	5
10^{15}	1130	1803	2584	3289	4046
10^{10}	923	1474	2107	2683	3297
10^{5}	653	1047	1484	1895	2319
	$W'^{(n)}$, $Z'^{(n)}$				
$z_L \backslash n$	1	2	3	4	5
10^{15}	1122	2576	4039	5503	6968
10^{10}	914	2097	3287	4479	5672
10^{5}	640	1469	2303	3139	3974
	$A^{\hat{4}(n)}$				
$z_L \backslash n$	1	2	3	4	5
10^{15}	1788	3274	4748	6218	7687
10^{10}	1456	2665	5061	6257	7451
10^{5}	1020	1867	2708	3547	4384

B. KK quarks and leptons

The mass eigenvalue equations for quarks (3.16) and (3.17) and similar equations for leptons contain the bulk mass parameters c_q, c_ℓ and the ratios $\tilde{\mu}^q/\mu_2^q$, $\tilde{\mu}^\ell/\mu_3^\ell$, which are determined such that their running masses are given in Table I. For the light quarks and leptons with $c > \frac{1}{2}$ the bulk mass parameters shift to larger values for smaller z_L, whereas for the heavy quarks with $c < \frac{1}{2}$ they become smaller. c_q, c_ℓ, $\tilde{\mu}^q/\mu_2^q$, and $\tilde{\mu}^\ell/\mu_3^\ell$ are tabulated in Table IX. We note that $\tilde{\mu}^\ell/\mu_3^\ell \ll 1$ as neutrino masses are very small.

The spectra of KK modes of quarks and leptons are determined by the same mass eigenvalue equations as the zero modes. They are tabulated in Table X. Except for the KK tower of (t, b), $u^{(n)}$ and $d^{(n)}$, for instance, have approximately degenerate masses. Similarly to the case of the gauge bosons, we find an inequality $m_{t^{(1)}} < m_{b^{(1)}} < m_{c^{(1)}} \simeq m_{s^{(1)}} < m_{d^{(1)}} \simeq m_{u^{(1)}}$.

VII. COUPLINGS OF KK GAUGE BOSONS

The couplings of quarks and leptons to KK gauge bosons can be calculated in the same manner as given in Sec. IV for the couplings to the 4D gauge bosons. As a general feature left-handed quarks and leptons are localized near the Planck brane, whereas right-handed ones near the TeV brane. KK gauge bosons are localized near the TeV brane so that right-handed quarks and leptons have larger couplings than left-handed ones. Because of this asymmetry the left-right symmetry is broken even in the strong interaction sector.

KK gluons do not decay into massless gluons. On the other hand, KK W and Z can decay into WZ and WW, respectively.

A. KK photons and gluons

The couplings of the first KK photon and gluon with quarks or leptons are tabulated in Table XI. The wave functions of the KK photon and gluon are the same and their couplings to quarks are the same up to a normalization factor. The largest coupling is $g_{u_R}^{G^{(1)}} \simeq g_{d_R}^{G^{(1)}}$. This is different from the other scenario in which the t quark dominantly couples to KK gluons.

We note that the couplings of right-handed fermions are so large that the perturbative treatment is not valid for the

TABLE IX. c and $\tilde{\mu}/\mu_2$ for quarks and leptons.

	c_q			c_ℓ		
z_L	(u, d)	(c, s)	(t, b)	(ν_e, e)	(ν_μ, μ)	(ν_τ, τ)
10^{15}	0.843	0.679	0.432	0.900	0.736	0.646
10^{10}	1.018	0.770	0.395	1.104	0.856	0.720
10^{5}	1.548	1.049	0.268	1.721	1.222	0.948
	$\tilde{\mu}^q/\mu_2^q$			$\mu_3^\ell/\tilde{\mu}^\ell$		
z_L	(u, d)	(c, s)	(t, b)	(ν_e, e)	(ν_μ, μ)	(ν_τ, τ)
10^{15}	2.283	0.0889	0.0173	4.87×10^8	1.14×10^{10}	3.47×10^{10}
10^{10}	2.283	0.0889	0.0175	4.87×10^8	1.14×10^{10}	3.47×10^{10}
10^{5}	2.283	0.0889	0.0181	4.87×10^8	1.14×10^{10}	3.47×10^{10}

TABLE X. The masses of KK quarks and leptons in units of GeV.

z_L	10^{15}	10^{10}	10^5
$u^{(1)}$, $d^{(1)}$	1361	1203	1037
$u^{(2)}$, $d^{(2)}$	2001	1716	1383
$u^{(3)}$, $d^{(3)}$	2823	2397	1886
$u^{(4)}$, $d^{(4)}$	3503	2944	2258
$u^{(5)}$, $d^{(5)}$	4287	3590	2727

z_L	10^{15}	10^{10}	10^5
$c^{(1)}$, $s^{(1)}$	1249	1068	855
$c^{(2)}$, $s^{(2)}$	1900	1593	1213
$c^{(3)}$, $s^{(3)}$	2706	2255	1692
$c^{(4)}$, $s^{(4)}$	3394	2812	2075
$c^{(5)}$, $s^{(5)}$	4169	3447	2529

z_L	10^{15}	10^{10}	10^5
$t^{(1)}$	1121	912	634
$t^{(2)}$	1797	1467	1037
$t^{(3)}$	2576	2097	1467
$t^{(4)}$	3279	2672	1877
$t^{(5)}$	4039	3287	2303

z_L	10^{15}	10^{10}	10^5
$b^{(1)}$	1172	975	734
$b^{(2)}$	1745	1402	936
$b^{(3)}$	2627	2160	1567
$b^{(4)}$	3228	2608	1778
$b^{(5)}$	4090	3351	2402

z_L	10^{15}	10^{10}	10^5
$\nu_e^{(1)}$, $e^{(1)}$, $\nu_\mu^{(1)}$, $\mu^{(1)}$, $\nu_\tau^{(1)}$, $\tau^{(1)}$	1400	1249	1099
$\nu_e^{(2)}$, $e^{(2)}$, $\nu_\mu^{(2)}$, $\mu^{(2)}$, $\nu_\tau^{(2)}$, $\tau^{(2)}$	2036	1758	1441
$\nu_e^{(3)}$, $e^{(3)}$, $\nu_\mu^{(3)}$, $\mu^{(3)}$, $\nu_\tau^{(3)}$, $\tau^{(3)}$	2863	2445	1952
$\nu_e^{(4)}$, $e^{(4)}$, $\nu_\mu^{(4)}$, $\mu^{(4)}$, $\nu_\tau^{(4)}$, $\tau^{(4)}$	3540	2990	2321
$\nu_e^{(5)}$, $e^{(5)}$, $\nu_\mu^{(5)}$, $\mu^{(5)}$, $\nu_\tau^{(5)}$, $\tau^{(5)}$	4328	3640	2794

KK gluons. With this reservation in mind one can evaluate the decay widths of the first KK gluon by using the couplings in Table XI. The decay width is given by

$$\Gamma(G^{(n)} \to f\bar{f}) = C\frac{\alpha_s m_{G^{(n)}}}{6} F(\bar{g}_{fL}^{G^{(n)}}, \bar{g}_{fR}^{G^{(n)}}, m_f, m_{G^{(n)}}), \tag{7.1}$$

where F is defined in (4.7) and $\bar{g}_{fL}^{G^{(n)}} = g_{fL}^{G^{(n)}}/(g_C/\sqrt{L})$. The color factor $C = 3$. Numerical values are tabulated in Table XII. It is found that the decay rate to the light quarks is large. The total decay width of $G^{(1)}$ turns out much larger than its mass. Thus the KK gluon cannot be identified as a resonance.

The decay width of the first KK photon $A^{\gamma(1)}$ is evaluated similarly. The decay width to a fermion pair is

TABLE XI. The couplings of the first KK photon to leptons and quarks, $g_f^{\gamma^{(1)}}/(g_A/\sqrt{L})$. $e = (g_A/\sqrt{L})\sin\theta_W$. The couplings of the first KK gluon to quarks, $g_f^{G^{(1)}}/(g_C/\sqrt{L})$, are the same as $g_f^{\gamma^{(1)}}/(g_A/\sqrt{L})$.

z_L	e_L	μ_L	τ_L	e_R	μ_R	τ_R
10^{15}	−0.195	−0.195	−0.195	6.408	6.147	5.981
10^{10}	−0.241	−0.241	−0.241	5.426	5.153	4.968
10^5	−0.347	−0.347	−0.346	4.123	3.872	3.672

z_L	u_L	c_L	t_L	u_R	c_R	t_R
10^{15}	−0.195	−0.195	0.442	6.323	6.044	5.603
10^{10}	−0.241	−0.241	0.554	5.339	5.040	4.497
10^5	−0.347	−0.347	0.890	4.049	3.753	2.925

z_L	d_L	s_L	b_L	d_R	s_R	b_R
10^{15}	−0.195	−0.195	0.661	6.323	6.044	5.500
10^{10}	−0.241	−0.241	0.797	5.339	5.040	4.376
10^5	−0.347	−0.347	1.111	4.049	3.753	2.786

$$\Gamma(\gamma^{(n)} \to f\bar{f}) = C\frac{q_f^2 \alpha m_{\gamma^{(n)}}}{3\sin^2\theta_W} F(\bar{g}_{fL}^{\gamma^{(n)}}, \bar{g}_{fR}^{\gamma^{(n)}}, m_f, m_{\gamma^{(n)}}), \tag{7.2}$$

where $\bar{g}_{fL}^{\gamma^{(n)}} = g_{fL}^{\gamma^{(n)}}/(g_A/\sqrt{L})$ and q_f is a charge $\frac{2}{3}$, $-\frac{1}{3}$, -1, 0. $C = 1$ for leptons.

In addition to decay into $q\bar{q}$ and $\ell\bar{\ell}$, the first KK photon can decay into W^+W^- through

$$\begin{aligned}
\mathcal{L}_{\rm int}^{WW\gamma^{(n)}} &= ig_{WW\gamma^{(n)}}\{(\partial_\mu W_\nu^\dagger - \partial_\nu W_\mu^\dagger)W^\mu A^{\gamma(n)\nu} \\
&\quad - (\partial_\mu W_\nu - \partial_\nu W_\mu)W^{\dagger\mu} A^{\gamma(n)\nu} \\
&\quad + (\partial_\mu A_\nu^{\gamma(n)} - \partial_\nu A_\mu^{\gamma(n)})W^{\dagger\mu} W^\nu\}, \\
g_{WW\gamma^{(n)}} &= g_A \int \frac{dz}{kz}\Big[h_{\gamma^{(n)}}^L \Big\{(h_W^L)^2 + \frac{1}{2}(h_W^\wedge)^2\Big\} \\
&\quad + h_{\gamma^{(n)}}^R \Big\{(h_W^R)^2 + \frac{1}{2}(h_W^\wedge)^2\Big\}\Big].
\end{aligned} \tag{7.3}$$

Inserting the mode functions in the Appendix, one finds

TABLE XII. First KK gluon decay: The branching fraction and the total width at the tree level without QCD corrections.

z_L	10^{15}	10^{10}	10^5
u (%)	18.68	19.40	20.88
d (%)	18.68	19.40	20.88
s (%)	17.07	17.29	17.96
c (%)	17.07	17.29	17.96
b (%)	14.33	13.44	11.38
t (%)	14.17	13.19	10.93
$\Gamma_{\rm total}$ (GeV)	7205	4070	1576
Mass (GeV)	1144	940	678

$$g_{WW\gamma^{(n)}} = \frac{e\sqrt{L}}{\sqrt{r_{\gamma^{(n)}}} r_W} \int \frac{dz}{kz} C(z;\lambda_{\gamma^{(n)}}) \{C(z;\lambda_W)^2 + \hat{S}(z;\lambda_W)^2\}. \tag{7.4}$$

Note that the photon coupling is universal; $g_{WW\gamma} = g_{WW\gamma^{(0)}} = e$. The first KK photon has a coupling $g_{WW\gamma^{(1)}}/e = (-0.056\,03, -0.067\,65, -0.091\,45)$ for $z_L = (10^{15}, 10^{10}, 10^5)$. The decay width is given by [56]

$$\Gamma(\gamma^{(n)} \to W^+W^-) = \frac{g^2_{WW\gamma^{(n)}} m_{\gamma^{(n)}}}{192\pi\eta_n^2}(1 + 20\eta_n + 12\eta_n^2)(1 - 4\eta_n)^{3/2}, \tag{7.5}$$

where $\eta_n = m_W^2/m^2_{\gamma^{(n)}}$.

The decay widths of the first KK photon are summarized in Table XIII. The observed mass m_W is used in the phase space of the final state in the evaluation of $\Gamma[\gamma^{(1)} \to W^+W^-]$. The first KK photon $A^{\gamma^{(1)}}$ has a total decay width larger than or comparable to its mass. It does not look like a resonance.

B. KK W and Z

The couplings of quarks and leptons to the first KK W boson are given in Table XIV. The quarks in the third generation have larger couplings than the other quarks and leptons. Couplings of right-handed quarks and leptons are rather small.

The fermion couplings of the first KK Z boson can be calculated similarly. They are tabulated in Table XV. The values of the couplings of left-handed leptons are not very sensitive to the generation. For a smaller warp factor, the magnitude of the couplings of left-handed (right-handed) leptons and quarks becomes larger (smaller). For left-handed leptons and quarks, the third generation has larger couplings than the first and second generations. In contrast, for right-handed leptons and quarks, the third generation has smaller couplings.

TABLE XIII. Branching fractions and decay widths of the first KK photon $\gamma^{(1)}$. $\alpha = 1/128$ is used.

z_L	10^{15}	10^{10}	10^5
e (%)	13.5	14.0	14.8
μ (%)	12.5	12.6	13.1
τ (%)	11.8	11.7	11.8
u (%)	18.2	18.8	19.8
c (%)	16.7	16.7	17.0
t (%)	13.8	12.8	10.4
d (%)	4.56	4.69	4.95
s (%)	4.16	4.18	4.26
b (%)	3.49	3.25	2.69
W (%)	1.30	1.28	1.23
Γ [all $f\bar{f}$] (GeV)	1933	1105	441
$\Gamma[W^+W^-]$ (GeV)	25.5	14.3	5.5
Γ_{total} (GeV)	1959	1120	446
Mass (GeV)	1144	940	678

TABLE XIV. The couplings of the first KK W boson with quarks and leptons, $g_f^{W^{(1)}}\sqrt{L}/g_A$.

z_L	$u_L d_L$	$c_L s_L$	$t_L b_L$
10^{15}	−0.138	−0.138	0.492
10^{10}	−0.170	−0.170	0.609
10^5	−0.244	−0.244	0.934

z_L	$e_L \nu_{eL}$	$\mu_L \nu_{\mu L}$	$\tau_L \nu_{\tau L}$
10^{15}	−0.138	−0.138	−0.138
10^{10}	−0.170	−0.170	−0.170
10^5	−0.244	−0.244	−0.244

z_L	$u_R d_R$	$c_R s_R$	$t_R b_R$
10^{15}	1.02×10^{-12}	1.08×10^{-8}	0.000 308
10^{10}	1.69×10^{-12}	1.88×10^{-8}	0.000 596
10^5	3.66×10^{-12}	4.55×10^{-8}	0.002 04

Just like KK photons KK Z bosons can decay into a pair of W bosons. Their couplings are given by

$$\begin{aligned}
\mathcal{L}_{\text{int}}^{WWZ^{(n)}} &= ig_{WWZ^{(n)}}\{(\partial_\mu W_\nu^\dagger - \partial_\nu W_\mu^\dagger)W^\mu Z^{(n)\nu} \\
&\quad - (\partial_\mu W_\nu - \partial_\nu W_\mu)W^{\dagger\mu} Z^{(n)\nu} \\
&\quad + (\partial_\mu Z_\nu^{(n)} - \partial_\nu Z_\mu^{(n)})W^{\dagger\mu} W^\nu\}, \\
g_{WWZ^{(n)}} &= g_A \int \frac{dz}{kz}\Big[h^L_{Z^{(n)}}\Big\{(h_W^L)^2 + \frac{1}{2}(h_W^\wedge)^2\Big\} \\
&\quad + h^R_{Z^{(n)}}\Big\{(h_W^R)^2 + \frac{1}{2}(h_W^\wedge)^2\Big\} + h^\wedge_{Z^{(n)}}\Big(h_W^L + h_W^R\Big)h_W^\wedge\Big],
\end{aligned} \tag{7.6}$$

where indices μ, ν are contracted with $\eta_{\mu\nu}$. With mode functions inserted,

$$\begin{aligned}
\frac{g_{WWZ^{(n)}}}{\frac{g_A}{\sqrt{L}}\cos\theta_W} &\equiv I_{WWZ^{(n)}} \\
&= \frac{\sqrt{L}}{\sqrt{2r_{Z^{(n)}}} r_W} \int \frac{dz}{kz}\Big[\frac{1 - 2\sin^2\theta_W}{\cos^2\theta_W} C(z;\lambda_{Z^{(n)}}) \\
&\quad \times \{C(z;\lambda_W)^2 + \hat{S}(z;\lambda_W)^2\} \\
&\quad + \frac{2}{\cos^2\theta_W}\hat{S}(z;\lambda_{Z^{(n)}})C(z;\lambda_W)\hat{S}(z;\lambda_W)\Big].
\end{aligned} \tag{7.7}$$

With the couplings $g_{WWZ^{(n)}}$ the partial decay width $\Gamma(Z^{(n)} \to W^+W^-)$ is given by the formula (7.5) where $g_{WW\gamma^{(n)}}$ and $m_{\gamma^{(n)}}$ are replaced by $g_{WWZ^{(n)}}$ and $m_{Z^{(n)}}$, respectively. The enhancement factor $1/\eta_n^2 = (m_{Z^{(n)}}/m_W)^4$ represents that $Z^{(n)}$ decays dominantly to the longitudinal components of W over the transverse components.

TABLE XV. The couplings of the first KK Z boson to leptons and quarks, $g_f^{Z^{(1)}}\sqrt{L}/g_A$.

z_L	ν_{eL}	$\nu_{\mu L}$	$\nu_{\tau L}$	ν_{eR}	$\nu_{\mu R}$	$\nu_{\tau R}$
10^{15}	−0.0577	−0.0577	−0.0576	1.1×10^{-31}	1.0×10^{-29}	3.5×10^{-28}
10^{10}	−0.0712	−0.0712	−0.0711	1.8×10^{-31}	1.7×10^{-29}	6.1×10^{-28}
10^{5}	−0.1025	−0.1025	−0.1023	3.8×10^{-31}	4.0×10^{-29}	1.5×10^{-27}

z_L	e_L	μ_L	τ_L	e_R	μ_R	τ_R
10^{15}	0.0311	0.0310	0.0311	2.516	2.420	2.352
10^{10}	0.0384	0.0383	0.0384	2.126	2.033	1.953
10^{5}	0.0557	0.0553	0.0558	1.598	1.531	1.436

z_L	u_L	c_L	t_L	u_R	c_R	t_R
10^{15}	−0.0400	−0.0400	−0.2058	−1.656	−1.585	−1.467
10^{10}	−0.0493	−0.0493	−0.2553	−1.396	−1.320	−1.174
10^{5}	−0.0713	−0.0713	−0.3814	−1.048	−0.977	−0.743

z_L	d_L	s_L	b_L	d_R	s_R	b_R
10^{15}	0.0488	0.0488	−0.5581	0.828	0.792	0.723
10^{10}	0.0602	0.0602	−0.6710	0.698	0.660	0.576
10^{5}	0.0869	0.0869	−0.9219	0.524	0.488	0.371

TABLE XVI. The couplings $WWZ^{(n)}$. The ratios $I_{WWZ^{(n)}} = g_{WWZ^{(n)}}/(g_A\cos\theta_W/\sqrt{L})$ are listed. $n=0$ corresponds to the WWZ coupling.

z_L	10^{15}	10^{10}	10^{5}
WWZ	0.999 85	0.999 66	0.998 62
$WWZ^{(1)}$	−0.0343	−0.0422	−0.0604
$WWZ^{(2)}$	2.07×10^{-5}	3.35×10^{-5}	5.42×10^{-5}
$WWZ^{(3)}$	-1.25×10^{-3}	-1.55×10^{-3}	-2.26×10^{-3}
$WWZ^{(4)}$	-1.38×10^{-5}	-2.59×10^{-5}	-7.76×10^{-5}
$WWZ^{(5)}$	-2.04×10^{-4}	-2.50×10^{-4}	-3.56×10^{-4}

TABLE XVII. First KK Z boson decay: The branching fractions and decay widths. $\alpha = 1/128$ is used.

z_L	10^{15}	10^{10}	10^{5}
e (%)	12.4	12.5	11.8
μ (%)	11.5	11.4	10.9
τ (%)	10.9	10.6	9.56
$\nu_e+\nu_\mu+\nu_\tau$ (%)	0.02	0.04	0.15
u (%)	16.7	16.8	15.9
c (%)	15.3	15.0	13.8
t (%)	12.9	11.9	9.51
d (%)	4.20	4.23	4.06
s (%)	3.85	3.79	3.55
b (%)	5.09	6.74	14.2
W (%)	7.10	6.96	6.51
$\Gamma[W^+W^-]$ (GeV)	30.0	17.0	6.8
$\Gamma_{\rm total}$ (GeV)	422	245	104
Mass (GeV)	1130	923	653

The numerical values of the couplings $g_{WWZ^{(n)}}$ are tabulated in Table XVI. $g_{WWZ} \equiv g_{WWZ^{(0)}}$ has been evaluated in [16]. There appears a tiny deviation in g_{WWZ} from that in the SM. The couplings of KK Z are found to be very small; $|g_{WWZ^{(n)}}| \ll g_{WWZ}$.

The decay width of the first KK Z boson is tabulated in Table XVII. The mass and total decay width of $Z^{(1)}$ are 1130 GeV and 422 GeV for $z_L = 10^{15}$, respectively. The branching fraction of the WW mode is about 7%. (The observed mass m_W is used in the phase space of the final state in the evaluation of $\Gamma[Z^{(1)} \to W^+W^-]$.) In contrast to the decay width of the Z boson given in Table VII, the decay rates for neutrinos in the first KK Z boson decay are very small.

VIII. SIGNALS OF KK Z AT THE TEVATRON AND LHC

The KK Z boson can be produced at the Tevatron and LHC. We first consider the production process of the first KK Z boson ($Z^{(1)}$) followed by its decay into an electron and a positron, $q\bar{q} \to Z^{(1)} \to e^+e^-$, as shown in Fig. 3. To this process the first KK photon ($A^{\gamma(1)}$) also contributes, which has a mass close to that of $Z^{(1)}$. Unlike $Z^{(1)}$, however, $A^{\gamma(1)}$ has a decay width larger than its mass so that its contribution is expected to give an additional smooth background to the $Z^{(1)}$ signal. Effects of KK particles such as $A^{\gamma(n)}$ ($n \geq 2$) are ignored in our analysis for simplicity, though they also give a smooth background. Our numerical calculation is done by MADGRAPH/MADEVENT [54] at the parton level with the CTEQ6L

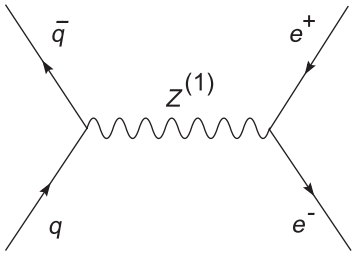

FIG. 3. The first KK Z boson signal.

parton distribution function [53] and without detector simulation.

The cross sections of $p\bar{p} \to e^+e^-X$ at $\sqrt{s} = 1.96$ TeV are evaluated as 22, 7.1, and 3.8 pb for $z_L = 10^5$, 10^{10}, and 10^{15}, respectively, where the invariant mass of the charged leptons is required to be larger than 150 GeV, and other cuts are the default values of MADGRAPH/MADEVENT: $p_T > 10$ GeV, $|\eta| < 2.5$, and $\Delta R > 0.4$ for the charged leptons. In the current model the production rate of $Z^{(1)}$ decreases for larger z_L as it becomes heavier. The background cross section, that is, the Drell-Yan cross section in the SM, is 0.73 pb. Including 10% theoretical uncertainty in the signal estimation, we obtain the statistical significance at the Tevatron with the integrated luminosity of 5.4(2.5) fb^{-1}, which corresponds to the analysis by D0 Collaboration [57] (CDF Collaboration [58]), as 9.7 (9.7), 9.0 (8.9), and 8.1(8.0) for $z_L = 10^5$, 10^{10}, and 10^{15}, respectively.

The first KK Z corresponds to what is referred to as Z' in the analysis of Tevatron data [57,58]. So far no signal of Z' has been found, which gives a constraint on the present model. The signals expected at the Tevatron are depicted in Fig. 4. A peak structure due to the first KK Z boson is seen in the case of $z_L = 10^5$, and thus the scenario with $z_L = 10^5$ is excluded. Furthermore, although the KK Z resonance shape is smeared out by the broad contribution of the first KK photon, the other scenarios with $z_L = 10^{10}$ and 10^{15} also seem disfavored by the present Tevatron data based only on the total cross section as stated above. If we take the detailed invariant mass distribution of the lepton pair and/or the dimuon channel into account, the limit on the warp factor will be strengthened.

As for LHC, we obtain the cross sections of $pp \to e^+e^-X$ at $\sqrt{s} = 7$ TeV as 91, 36, and 20 pb for $z_L = 10^5$, 10^{10}, and 10^{15}, respectively, and 1.8 pb for the SM. The same cuts on the final state as the $p\bar{p}$ case are applied.

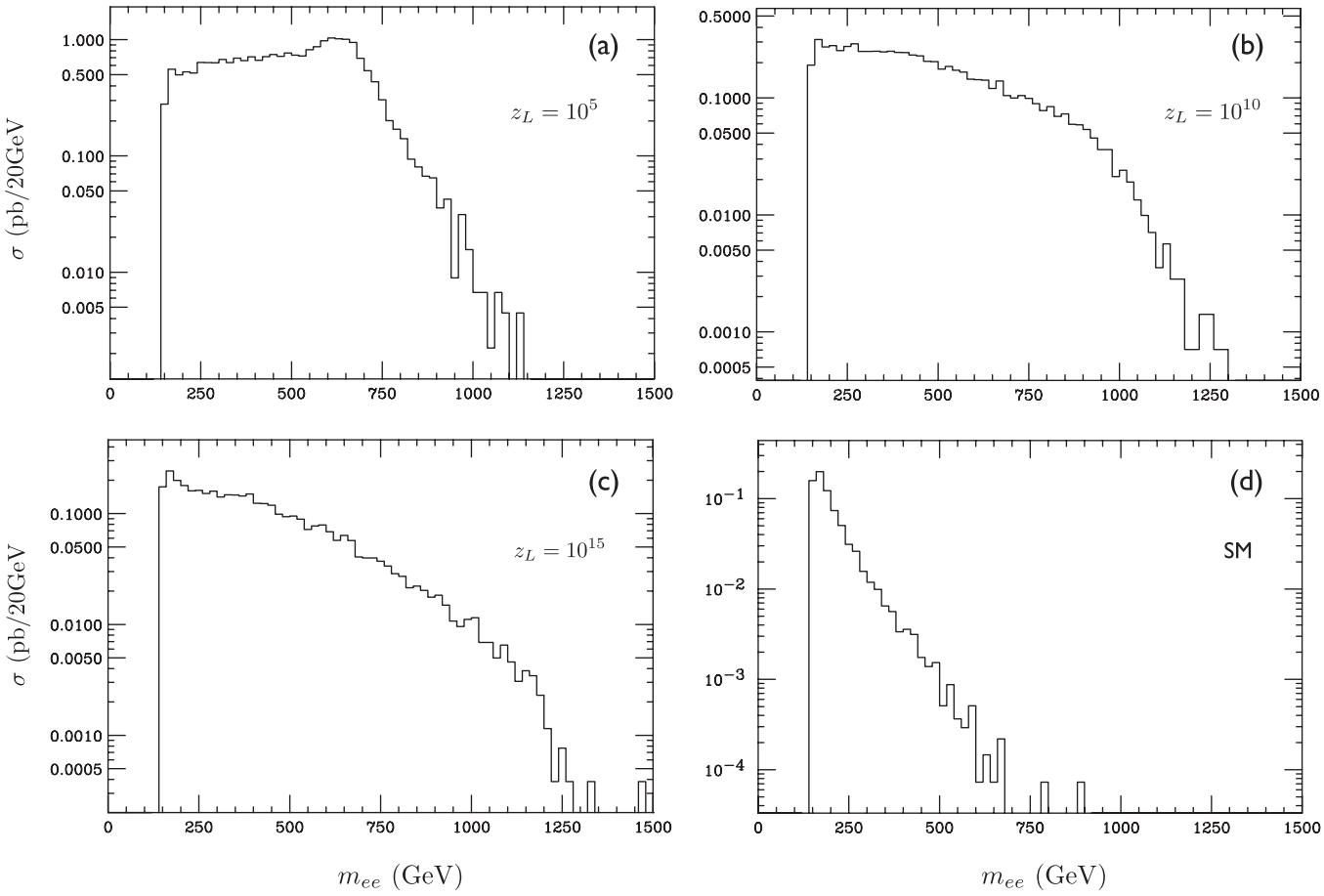

FIG. 4. Distributions of the e^+e^- invariant mass in $p\bar{p} \to e^+e^-X$ at $\sqrt{s} = 1.96$ TeV. (a) The present model with $z_L = 10^5$. (b) $z_L = 10^{10}$. (c) $z_L = 10^{15}$. (d) The SM.

TABLE XVIII. Significance of $pp \to e^+e^-X$ at $\sqrt{s} = 7$ TeV.

z_L	10^5	10^{10}	10^{15}
$L = 35$ pb^{-1}	9.7	9.1	8.5
$L = 100$ pb^{-1}	9.7	9.4	8.9
$L = 1000$ pb^{-1}	9.8	9.5	9.1

The statistical significance at LHC is summarized in Table XVIII, where 10% theoretical uncertainty is assumed. The signals expected at LHC are shown in Fig. 5. The resonant structure of the first KK Z boson remains for all the three values of z_L.

Recently, CMS and ATLAS Collaborations have searched for narrow resonances in dilepton channels and found no significant deviation from the SM [59,60]. The integrated luminosity for the electron channel is reported as 35 pb^{-1} by CMS and 39 pb^{-1} by ATLAS. Accordingly, the cases that $z_L \lesssim 10^{15}$ seem unlikely although we need a detailed analysis to determine the excluded parameter region. It should be noted that the total decay width of the first KK Z is very large in the current model, whereas a narrow width (3% of its mass or less) has been assumed in the analysis in Refs. [59,60].

We comment that contributions from higher KK photons $A^{\gamma(n)}$ ($n \geq 2$), which have broad decay widths, may have destructive interference with that from the first KK photon so that the magnitude of the smooth background is significantly decreased. If this is the case, the bound from the current data at the Tevatron and at LHC is weakened. More thorough study is necessary on this respect, which is reserved for the future.

As seen in Tables XI and XV, the couplings of $A^{\gamma(1)}$ and $Z^{(1)}$ to the right-handed fermions except the neutrinos and the bottom quark are significantly larger than those to the left-handed fermions. Such a parity violation affects the distribution of the leptons in the final state. Consider a favored parton-parton collision, for instance, $u_R\bar{u}_R \to e_R^-e_R^+$. The direction of the final e_R^- tends to be that of the initial u_R because of the helicity conservation. This angular distribution in the parton center-of-mass frame results in a harder electron spectrum (and a softer positron spectrum) in the pp center-of-mass frame since most of the initial quark-antiquark pairs are boosted in the direction of

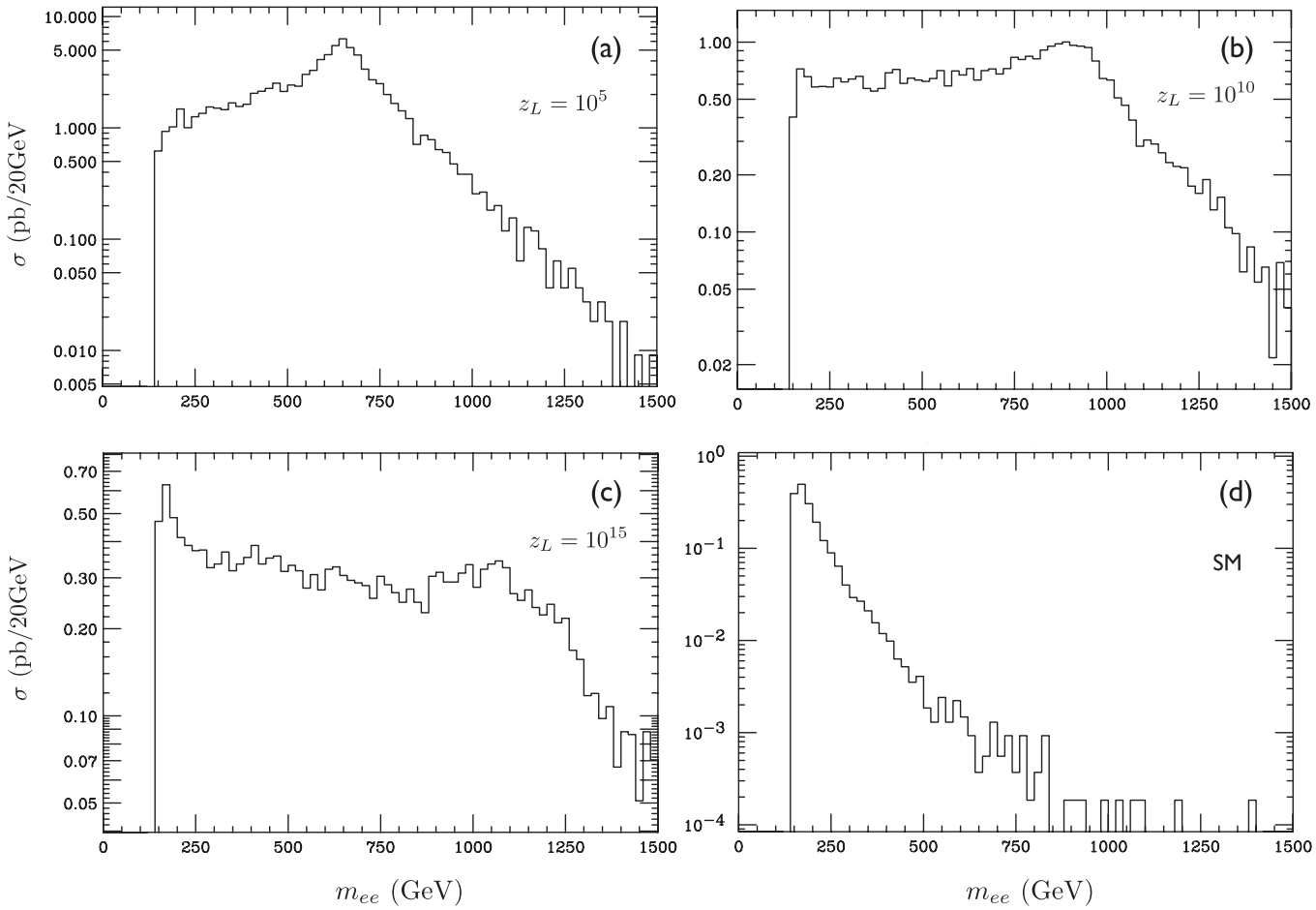

FIG. 5. Distributions of the e^+e^- invariant mass in $pp \to e^+e^-X$ at $\sqrt{s} = 7$ TeV. (a) The present model with $z_L = 10^5$. (b) $z_L = 10^{10}$. (c) $z_L = 10^{15}$. (d) The SM.

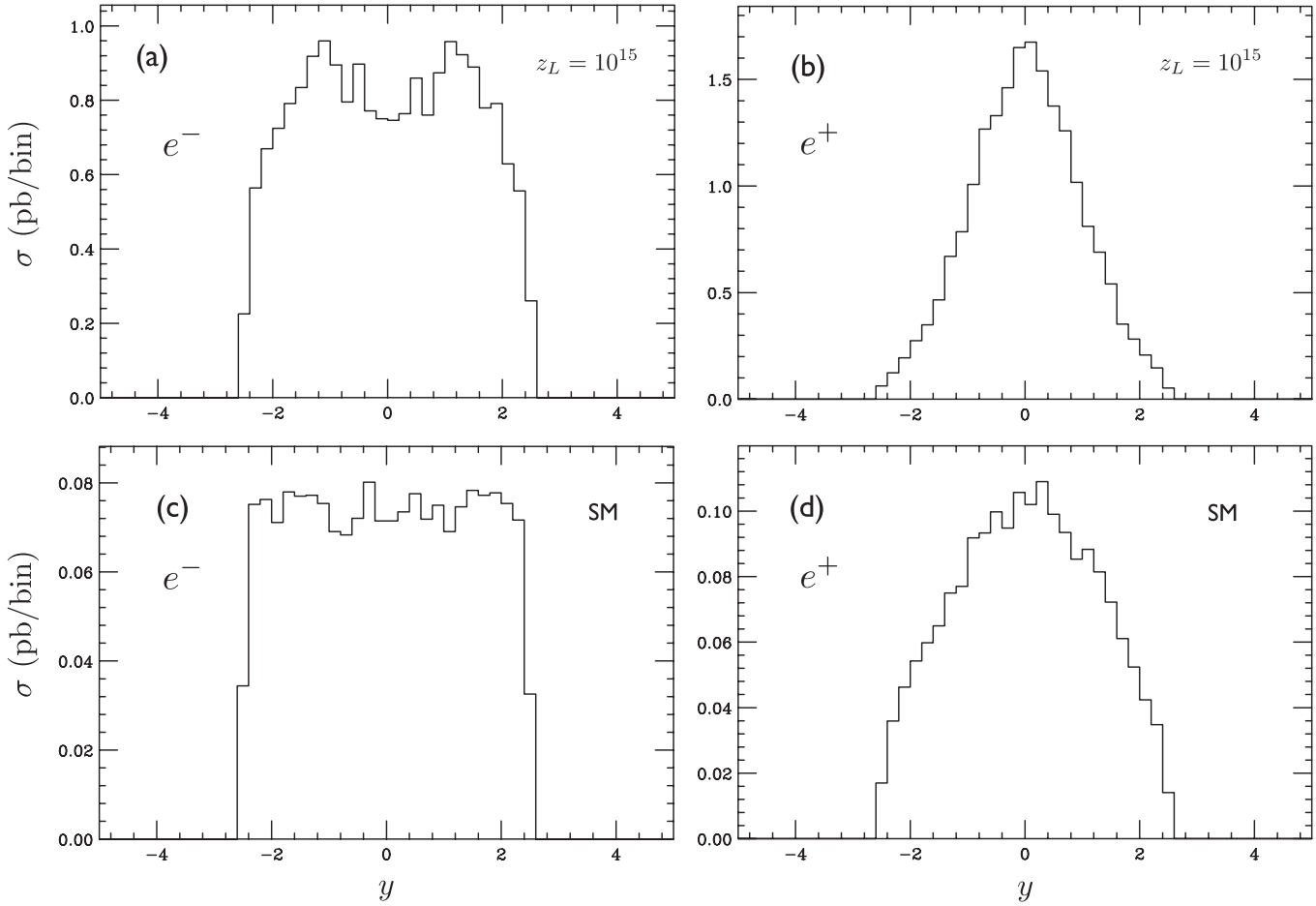

FIG. 6. The rapidity distributions. (a) The electron distribution in the present model with $z_L = 10^{15}$. (b) The positron distribution in the present model with $z_L = 10^{15}$. (c) The electron distribution in the SM. (d) The positron distribution in the SM.

the initial quark in the pp collider. Hence, we expect a wider rapidity distribution for the electron than the positron. We present, in Fig. 6, the rapidity (y) distributions of the electron and positron in the present model with $z_L = 10^{15}$ and in the SM. Though both the models have the similar tendency that the electron distribution is wider than the positron, the difference between the electron and the positron is more significant in the present model. This feature in the rapidity distributions is quantified by the central charge asymmetry [61],

$$A_{cc}(y_c) = \frac{\sigma(|y_{e^-}| < y_c) - \sigma(|y_{e^+}| < y_c)}{\sigma(|y_{e^-}| < y_c) + \sigma(|y_{e^+}| < y_c)}. \qquad (8.1)$$

Our numerical study suggests that the statistical significance of $A_{cc}(y_c)$ is maximized with $y_c \sim 0.6$ for the case of $z_L = 10^{15}$. We find that $A_{cc}(0.6) = -0.32(-0.17)$ for $z_L = 10^{15}$ (the SM) and the significance of 5σ is expected with the integrated luminosity of about 1 fb^{-1}. Another signal of the parity violation may be seen in the lepton forward-backward asymmetry with respect to the boost direction of the KK Z boson [62,63].

TABLE XIX. Significance of $pp \to je^+e^-X$ at $\sqrt{s} = 7$ TeV.

z_L	10^5	10^{10}	10^{15}
$L = 35$ pb^{-1}	9.5	8.9	8.1
$L = 100$ pb^{-1}	9.7	9.3	8.8
$L = 1000$ pb^{-1}	9.8	9.6	9.2

We also evaluate the cross section of $pp \to je^+e^-X$ at $\sqrt{s} = 7$ TeV, where j denotes a jet, to find 43, 17, and 9.3 pb for $z_L = 10^5$, 10^{10}, and 10^{15}, respectively. The same cuts on the final leptons as the $pp \to e^+e^-X$ case are applied, and the default cuts for jets in MADGRAPH/MADEVENT, that is, $p_T > 20$ GeV, $|\eta| < 5$, and $\Delta R > 0.4$ for the jet, are employed. Approximately 80% of the cross section for $z_L = 10^{15}$ includes a gluon jet ($q\bar{q} \to gZ^{(1)}$, $gA^{\gamma(1)}$) and the rest does a quark jet ($qg \to qZ^{(1)}$, $qA^{\gamma(1)}$). The SM cross section is estimated to be 0.66 pb. The statistical significance assuming 10% theoretical uncertainty is shown in Table XIX. The $pp \to je^+e^-X$ mode has a comparable sensitivity of the $pp \to e^+e^-X$ mode from the statistical point of view, but the background should be studied carefully since the signal is more complicated.

IX. CONCLUSIONS

In the present paper we have explored collider signatures of the $SO(5) \times U(1)$ gauge-Higgs unification model in the RS space. The model predicts $\theta_H = \frac{1}{2}\pi$ and the stable Higgs boson. The gauge and Higgs couplings of quarks and leptons deviate from those in the standard model. With the warp factor z_L given, the mass spectra and couplings of all fields are determined.

There arises small deviation in the gauge couplings of quarks and leptons. This leads to forward-backward asymmetry in e^+e^- annihilation on the Z resonance. It was found that the gauge-Higgs unification model gives good fit to the forward-backward asymmetry data in a wide rage of z_L. However, the data of branching fractions of various modes in the Z boson decay fit well only for $z_L \gtrsim 10^{15}$.

Pair production of Higgs bosons at ILC, $e^+e^- \to ZHH$, is marginal. There is a large background containing neutrinos. With polarized beam and appropriate cut, the statistical significance S of the signal is estimated to be $S/\sqrt{L(\text{fb}^{-1})} = 0.11$ for $\sqrt{s} = 750$ GeV for $z_L = 10^{15}$, which requires the luminosity $L > 2.0\ \text{ab}^{-1}$ for 5σ discovery.

Another important way to test the model is to produce KK modes. The production of the first KK Z boson $Z^{(1)}$ decaying into e^+e^- gives a clear signal. At $z_L = 10^{15}$ the mass and width of $Z^{(1)}$ are about 1130 GeV and 422 GeV, respectively. The production of $Z^{(1)}$ can be discovered at LHC through $pp \to Z^{(1)}X \to e^+e^-X$ with 100 pb^{-1}. There appears a smooth background coming from the production and decay of KK photons. The mass and width of the first KK photon $A^{\gamma(1)}$ are 1144 GeV and 1959 GeV at $z_L = 10^{15}$, respectively. We have evaluated the cross section including the contribution from $A^{\gamma(1)}$. The present limit from the Z' searches at the Tevatron and LHC excludes $z_L \lesssim 10^{15}$. However, a more thorough study taking account of contributions of higher KK photons $A^{\gamma(n)}$ $(n \geq 2)$ is necessary, as destructive interference could occur in the smooth background.

It is a general feature that KK gluons, photons, and Z couple dominantly to right-handed quarks and leptons. The large parity violation affects the rapidity distributions of e^+ and e^- in the decay of $Z^{(1)}$, which is quantified by measuring the central charge asymmetry.

We conclude that the present precision data of the gauge couplings and Z' search indicate a large warp factor $z_L > 10^{15}$. $Z^{(1)}$ production at LHC is a promising way to test the model.

In the present paper we have investigated the $SO(5) \times U(1)$ gauge-Higgs model with bulk fermions in the vector representation of $SO(5)$, in which right-handed quarks and leptons are localized near the TeV brane and have large couplings with KK gauge bosons. It would be interesting to see whether the couplings of the leptons to the KK photons can be suppressed by introducing bulk lepton multiplets in another tensorial representation of $SO(5)$.

It has been shown that in order for the stable Higgs boson to account for the dark matter of the Universe, its mass must be $m_H \sim 70$ GeV, which is obtained with a small warp factor $z_L \sim 10^5$ in the current model. Further improvement of the model is necessary to explain both collider data and dark matter.

ACKNOWLEDGMENTS

The authors would like to thank C. Csaki, N. Haba, S. Kanemura, and S. Matsumoto for many valuable comments. This work was supported in part by scientific grants from the Ministry of Education and Science, Grants No. 20244028 (Y. H., N. U.), No. 21244036 (Y. H.), and No. 20244037 (M. T.).

APPENDIX: NORMALIZED MODE FUNCTIONS

In this appendix, mode functions with their normalization factors at $\theta_H = \frac{1}{2}\pi$ are collected [18]. Basis functions are given in (3.5) and (3.13). For convenience we define

$$\hat{S}(z;\lambda) = \frac{C(1;\lambda)}{S(1;\lambda)} S(z;\lambda),$$
$$\hat{S}_L(z;\lambda,c) = \frac{C_L(1;\lambda,c)}{S_L(1;\lambda,c)} S_L(z;\lambda,c). \tag{A1}$$

1. Gauge bosons

Gauge bosons are expanded as in (3.12). Mode functions $h(z)$ of P_H-even fields, for instance, satisfy orthogonality conditions

$$\int_1^{z_L} \frac{dz}{kz} \{h^L_{W^{(n)}} h^L_{W^{(m)}} + h^R_{W^{(n)}} h^R_{W^{(m)}} + h^{\wedge}_{W^{(n)}} h^{\wedge}_{W^{(m)}}\} = \delta^{nm},$$
$$\int_1^{z_L} \frac{dz}{kz} \{h^L_{Z^{(n)}} h^L_{Z^{(m)}} + h^R_{Z^{(n)}} h^R_{Z^{(m)}} + h^{\wedge}_{Z^{(n)}} h^{\wedge}_{Z^{(m)}} + h^B_{Z^{(n)}} h^B_{Z^{(m)}}\} = \delta^{nm},$$
$$\int_1^{z_L} \frac{dz}{kz} \{h^L_{\gamma^{(n)}} h^L_{\gamma^{(m)}} + h^R_{\gamma^{(n)}} h^R_{\gamma^{(m)}} + h^B_{\gamma^{(n)}} h^B_{\gamma^{(m)}}\} = \delta^{nm},$$
$$\int_1^{z_L} \frac{dz}{kz} \{h^L_{Z^{(n)}} h^L_{\gamma^{(m)}} + h^R_{Z^{(n)}} h^R_{\gamma^{(m)}} + h^B_{Z^{(n)}} h^B_{\gamma^{(m)}}\} = 0. \tag{A2}$$

Similar relations hold for other mode functions.

(i) Photon tower $(\hat{A}^{\gamma}_{\mu})$

$$h^L_{\gamma^{(n)}} = h^R_{\gamma^{(n)}} = \frac{s_\phi}{\sqrt{1+s_\phi^2}} \frac{1}{\sqrt{r_{\gamma^{(n)}}}} C(z;\lambda_{\gamma^{(n)}}),$$
$$h^B_{\gamma^{(n)}} = \frac{c_\phi}{\sqrt{1+s_\phi^2}} \frac{1}{\sqrt{r_{\gamma^{(n)}}}} C(z;\lambda_{\gamma^{(n)}}), \tag{A3}$$
$$r_{\gamma^{(n)}} = \int_1^{z_L} \frac{dz}{kz} C(z;\lambda_{\gamma^{(n)}})^2.$$

For a photon $C(z;\lambda_{\gamma^{(0)}}=0)=\text{const}=\sqrt{r_{\gamma^{(0)}}/L}$.

Note that $s_\phi=\tan\theta_W$ and $1/\sqrt{1+s_\phi^2}=\cos\theta_W$.

(ii) W boson tower ($\hat{W}_\mu$)

$$\begin{aligned} h^L_{W^{(n)}} &= h^R_{W^{(n)}} = \frac{1}{\sqrt{2r_{W^{(n)}}}} C(z;\lambda_{W^{(n)}}),\\ h^{\wedge}_{W^{(n)}} &= -\frac{1}{\sqrt{r_{W^{(n)}}}} \hat{S}(z;\lambda_{W^{(n)}}),\\ r_{W^{(n)}} &= \int_1^{z_L} \frac{dz}{kz}\{C(z;\lambda_{W^{(n)}})^2 + \hat{S}(z;\lambda_{W^{(n)}})^2\}. \end{aligned} \tag{A4}$$

(iii) Z boson tower ($\hat{Z}_\mu$)

$$\begin{aligned} h^L_{Z^{(n)}} = h^R_{Z^{(n)}} &= \frac{c_\phi^2}{\sqrt{1+s_\phi^2}} \frac{1}{\sqrt{2r_{Z^{(n)}}}} C(z;\lambda_{Z^{(n)}})\\ &= \frac{1-2\sin^2\theta_W}{\cos\theta_W} \frac{C(z;\lambda_{Z^{(n)}})}{\sqrt{2r_{Z^{(n)}}}},\\ h^{\wedge}_{Z^{(n)}} &= -\sqrt{1+s_\phi^2} \frac{1}{\sqrt{r_{Z^{(n)}}}} \hat{S}(z;\lambda_{Z^{(n)}})\\ &= -\frac{1}{\cos\theta_W} \frac{\hat{S}(z;\lambda_{Z^{(n)}})}{\sqrt{r_{Z^{(n)}}}},\\ h^B_{Z^{(n)}} &= -\frac{\sqrt{2}s_\phi c_\phi}{\sqrt{1+s_\phi^2}} \frac{1}{\sqrt{r_{Z^{(n)}}}} C(z;\lambda_{Z^{(n)}})\\ &= -\frac{g_A}{g_B} \frac{\sin^2\theta_W}{\cos\theta_W} \frac{\sqrt{2}C(z;\lambda_{Z^{(n)}})}{\sqrt{r_{Z^{(n)}}}},\\ r_{Z^{(n)}} &= \int_1^{z_L} \frac{dz}{kz}\{c_\phi^2 C(z;\lambda_{Z^{(n)}})^2 + (1+s_\phi^2)\hat{S}(z;\lambda_{Z^{(n)}})^2\}. \end{aligned} \tag{A5}$$

(iv) $\hat{W}'_\mu$ tower

$$\begin{aligned} h^L_{W'^{(n)}} &= -h^R_{W'^{(n)}} = \frac{1}{\sqrt{2}} \frac{1}{\sqrt{r_{W'^{(n)}}}} C(z;\lambda_{W'^{(n)}}),\\ r_{W'^{(n)}} &= \int_1^{z_L} \frac{dz}{kz} C(z;\lambda_{W'^{(n)}})^2. \end{aligned} \tag{A6}$$

(v) $\hat{Z}'_\mu$ tower

$$\begin{aligned} h^L_{Z'^{(n)}} &= -h^R_{Z'^{(n)}} = \frac{1}{\sqrt{2}} \frac{1}{\sqrt{r_{Z'^{(n)}}}} C(z;\lambda_{Z'^{(n)}}),\\ r_{Z'^{(n)}} &= \int_1^{z_L} \frac{dz}{kz} C(z;\lambda_{Z'^{(n)}})^2. \end{aligned} \tag{A7}$$

(vi) $\hat{A}^{\hat{4}}_\mu$ tower

$$\begin{aligned} h_{A^{(n)}} &= \frac{1}{\sqrt{r_{A^{\hat{4}(n)}}}} S(z;\lambda_{A^{\hat{4}(n)}}),\\ r_{A^{\hat{4}(n)}} &= \int_1^{z_L} \frac{dz}{kz} S(z;\lambda_{A^{\hat{4}(n)}})^2. \end{aligned} \tag{A8}$$

The mode functions for the fifth-dimensional component are given similarly. h^{LR}_S, h^{LR}_D, $h_B \propto C'(z;\lambda)$ and $h^{\wedge}_H$, $h^{\wedge}_D \propto S'(z;\lambda)$. The normalization condition is given by $\int_1^{z_L}(kdz/z)(h_s)^2=1$ where $h_s = h^{LR}_S$, $h^{\wedge}_H$, h^{LR}_D, $h^{\wedge}_D$, h_B.

2. Fermions

For P_H-even $\psi^{(n)}_{(2/3)(+)}$, Eq. (3.14) leads to

$$[a^{(n)}_U, a^{(n)}_{t'}] \simeq \left[-\frac{\sqrt{2}\tilde{\mu}}{\mu_2}, -\frac{C_L(1;\lambda_n,c_t)}{S_L(1;\lambda_n,c_t)}\right] a^{(n)}_{B+t}. \tag{A9}$$

With this ratio, the coefficient is given by

$$a^{(n)}_{B+t} = \left[\int_1^{z_L} dz \left\{\left[2\left(\frac{\tilde{\mu}}{\mu_2}\right)^2 + 1\right] C_L(z;\lambda_n,c_t)^2 + \hat{S}_L(z;\lambda_n,c_t)^2\right\}\right]^{-1/2}. \tag{A10}$$

For P_H-odd $t^{(n)}_{(-)}$, the coefficient is

$$a^{(n)}_{B-t} = \left[\int_1^{z_L} dz C_L(z;\lambda_{t^{(n)}_{(-)}},c_t)^2\right]^{-1/2}. \tag{A11}$$

For P_H-even $\psi^{(n)}_{-(1/3)(+)}$, the coefficients satisfy

$$[a^{(n)}_b, a^{(n)}_{b'}] \simeq \left[-\frac{\sqrt{2}\mu_2}{\tilde{\mu}}, -\frac{C_L(1;\lambda_n,c_t)}{S_L(1;\lambda_n,c_t)}\right] a^{(n)}_{D+X}, \tag{A12}$$

which yields

$$a^{(n)}_{D+X} = \left[\int_1^{z_L} dz \left\{\left[2\left(\frac{\mu_2}{\tilde{\mu}}\right)^2 + 1\right] C_L(z;\lambda_n,c_t)^2 + \hat{S}_L(z;\lambda_n,c_t)^2\right\}\right]^{-1/2}. \tag{A13}$$

For P_H-odd $b^{(n)}_{(-)}$, the coefficient is given by

$$a^{(n)}_{D-X} = \left[\int_1^{z_L} dz C_L(z;\lambda_{b^{(n)}_{(-)}},c_t)^2\right]^{-1/2}. \tag{A14}$$

To obtain overlap integrals for the gauge couplings, these normalization constants are taken into account.

[1] C. Csaki, C. Grojean, H. Murayama, L. Pilo, and J. Terning, Phys. Rev. D **69**, 055006 (2004).
[2] G. Cacciapaglia, C. Csaki, C. Grojean, and J. Terning, Phys. Rev. D **70**, 075014 (2004).
[3] N. Arkani-Hamed, A. G. Cohen, and H. Georgi, Phys. Lett. B **513**, 232 (2001).
[4] D. E. Kaplan and M. Schmaltz, J. High Energy Phys. 10 (2003) 039.
[5] M. Schmaltz and D. Tucker-Smith, Annu. Rev. Nucl. Part. Sci. **55**, 229 (2005).
[6] Y. Hosotani, Phys. Lett. **126B**, 309 (1983).
[7] A. T. Davies and A. McLachlan, Phys. Lett. B **200**, 305 (1988)
[8] Y. Hosotani, Ann. Phys. (N.Y.) **190**, 233 (1989).
[9] H. Hatanaka, T. Inami, and C. S. Lim, Mod. Phys. Lett. A **13**, 2601 (1998).
[10] C. A. Scrucca, M. Serone, and L. Silvestrini, Nucl. Phys. **B669**, 128 (2003).
[11] G. Burdman and Y. Nomura, Nucl. Phys. **B656**, 3 (2003).
[12] C. Csaki, C. Grojean, and H. Murayama, Phys. Rev. D **67**, 085012 (2003).
[13] K. Agashe, R. Contino, and A. Pomarol, Nucl. Phys. **B719**, 165 (2005).
[14] A. D. Medina, N. R. Shah, and C. E. M. Wagner, Phys. Rev. D **76**, 095010 (2007).
[15] Y. Sakamura and Y. Hosotani, Phys. Lett. B **645**, 442 (2007).
[16] Y. Hosotani and Y. Sakamura, Prog. Theor. Phys. **118**, 935 (2007).
[17] Y. Hosotani, K. Oda, T. Ohnuma, and Y. Sakamura, Phys. Rev. D **78**, 096002 (2008); **79**, 079902(E) (2009).
[18] Y. Hosotani, S. Noda, and N. Uekusa, Prog. Theor. Phys. **123**, 757 (2010).
[19] Y. Hosotani, P. Ko, and M. Tanaka, Phys. Lett. B **680**, 179 (2009).
[20] Y. Hosotani, M. Tanaka, and N. Uekusa, Phys. Rev. D **82**, 115024 (2010).
[21] K. Cheung and J. Song, Phys. Rev. D **81**, 097703 (2010); **81**, 119905(E) (2010).
[22] A. Alves, Phys. Rev. D **82**, 115021 (2010).
[23] R. Contino, Y. Nomura, and A. Pomarol, Nucl. Phys. **B671**, 148 (2003).
[24] T. Gherghetta, arXiv:1008.2570.
[25] N. G. Deshpande and E. Ma, Phys. Rev. D **18**, 2574 (1978).
[26] E. Ma, Phys. Rev. D **73**, 077301 (2006).
[27] R. Barbieri, L. J. Hall, and V. S. Rychkov, Phys. Rev. D **74**, 015007 (2006).
[28] Q-H. Cao, E. Ma, and G. Rajasekaran, Phys. Rev. D **76**, 095011 (2007).
[29] K. Agashe and R. Contino, Nucl. Phys. **B742**, 59 (2006).
[30] G. Cacciapaglia, C. Csaki, and S. C. Park, J. High Energy Phys. 03 (2006) 099.
[31] Y. Hosotani, S. Noda, Y. Sakamura, and S. Shimasaki, Phys. Rev. D **73**, 096006 (2006).
[32] K. Agashe, R. Contino, L. Da Rold, and A. Pomarol, Phys. Lett. B **641**, 62 (2006).
[33] C. S. Lim and N. Maru, Phys. Rev. D **75**, 115011 (2007).
[34] M. S. Carena, E. Ponton, J. Santiago, and C. E. M. Wagner, Phys. Rev. D **76**, 035006 (2007).
[35] G. F. Giudice, C. Grojean, A. Pomarol, and R. Rattazzi, J. High Energy Phys. 06 (2007) 045.
[36] Y. Sakamura, Phys. Rev. D **76**, 065002 (2007).
[37] Y. Adachi, C. S. Lim, and N. Maru, Phys. Rev. D **76**, 075009 (2007).
[38] M. Carena, A. D. Medina, B. Panes, N. R. Shah, and C. E. M. Wagner, Phys. Rev. D **77**, 076003 (2008).
[39] Y. Hosotani and Y. Kobayashi, Phys. Lett. B **674**, 192 (2009).
[40] B. Gripaios, A. Pomarol, F. Riva, and J. Serra, J. High Energy Phys. 04 (2009) 070.
[41] Y. Adachi, C. S. Lim, and N. Maru, Phys. Rev. D **80**, 055025 (2009).
[42] K. Agashe, A. Azatov, T. Han, Y. Li, Z. G. Si, and L. Zhu, Phys. Rev. D **81**, 096002 (2010).
[43] N. Uekusa, arXiv:0912.1218.
[44] N. Maru and Y. Sakamura, J. High Energy Phys. 04 (2010) 100.
[45] Y. Sakamura, Phys. Rev. D **83**, 036007 (2011).
[46] N. Haba, K. Oda, and R. Takahashi, J. High Energy Phys. 05 (2011) 125.
[47] N. Haba, M. Harada, Y. Hosotani, and Y. Kawamura, Nucl. Phys. **B657**, 169 (2003); **B669**, 381 (2003).
[48] N. Haba, Y. Hosotani, and Y. Kawamura, Prog. Theor. Phys. **111**, 265 (2004).
[49] Z. z. Xing, H. Zhang, and S. Zhou, Phys. Rev. D **77**, 113016 (2008).
[50] C. Amsler *et al.* (Particle Data Group), Phys. Lett. B **667**, 1 (2008).
[51] Y. Hosotani, arXiv:hep-ph/0303066.
[52] O. J. P. Éboli and D. Zeppenfeld, Phys. Lett. B **495**, 147 (2000).
[53] J. Pumplin *et al.*, J. High Energy Phys. 07 (2002) 012.
[54] J. Alwall *et al.*, J. High Energy Phys. 09 (2007) 028.
[55] T. Ishikawa *et al.* (MINAMI-TATEYA Collaboration) [http://www-sc.kek.jp/].
[56] F. del Aguila, M. Quiros, and F. Zwirner, Nucl. Phys. **B284**, 530 (1987).
[57] D0 Collaboration, Phys. Lett. B **695**, 88 (2011).
[58] T. Aaltonen *et al.* (CDF Collaboration), Phys. Rev. Lett. **102**, 031801 (2009).
[59] CMS Collaboration, J. High Energy Phys. 05 (2011) 093.
[60] ATLAS Collaboration, Phys. Lett. B **700**, 163 (2011).
[61] O. Antuñano, J. H. Kühn, and G. Rodrigo, Phys. Rev. D **77**, 014003 (2008).
[62] M. Dittmar, Phys. Rev. D **55**, 161 (1997).
[63] M. Dittmar, A.-S. Nicollert, and A. Djouadi, Phys. Lett. B **583**, 111 (2004).